Identification of time-varying cable forces based on parameter optimization variational mode decomposition

Final Project

Facultad de Náutica de Barcelona

Universidad Politécnica de Cataluña

Author:

Junfeng Xu

Director:

Martinez Garcia Javier

Zhimin Feng

NAVAL AND OCEAN ENGINEERING

Barcelona, July 2020

ABSTRACT

Accumulated fatigue damage is one of the main causes of damage and destruction of actual bridge structures. For cable bridges, the cable is the key force component. The cumulative fatigue damage of the cable seriously threatens the safety of the bridge structure. The traditional cable force test based on the vibration method can only identify the average cable force of a bridge cable over a period of time. However, due to vehicle load and environmental factors, the cable force of the bridge cable is time-varying. Time-varying cable force is the main cause of fatigue damage, and it is also the basis for the safety assessment of cable limit state and the evaluation of cumulative fatigue damage. To this end, this paper studies the identification method of bridge cable time-varying cable force based on variational mode decomposition.

The main research contents of this article include:

Based on the time-frequency analysis method of variational mode decomposition, a new method for identifying time-varying cable forces is proposed. The time-frequency analysis method of variational modal decomposition is a new development method in the field of current signal processing. Its principle is to obtain a limited number of IMF and extract the instantaneous frequency of the time-varying system by performing Hilbert transform on the obtained IMF. Firstly, according to the time-frequency analysis method of variational modal decomposition, the time-varying modal frequency is identified from the measured cable acceleration. Then, the bridge cable is simplified into an ideal tension string, and the cable force is identified based on the relationship between the cable force and frequency established by the classic string vibration theory. The frequency-doubling relationship of the vibration of the cable is used to reduce the optimization variables of the method, improve the calculation efficiency, reduce the influence of noise on the different instantaneous frequencies of the cable, and improve the accuracy of

frequency identification of time-varying modal. Finally, the time-varying modal frequency of the identified cable is substituted into the cable force formula to obtain the time-varying cable force of the cable.

In the practical application of variational modal decomposition, the choice of penalty factors and the number of components has a great influence on the final signal decomposition results. In order to automatically determine the best parameter combination, the particle swarm optimization algorithm is used to search for these two influencing parameters in parallel . Simulation signal and engineering signal processing results show that the proposed method can achieve identification of time-varying frequency.

For the end effect of the instantaneous frequency curve, the signal extension method is used. Reduce the error of the instantaneous frequency at the end point. Design and build a tilting cable vibration test platform, and compare the test results with the calculation results to further verify the correctness of the method in this paper. The results show that the cable force error is about ± 5.0%.

Keywords: structural health monitoring; time-varying cable forces; variational modal decomposition; particle swarm optimization

Acknowledgements

To be honest, a year of FNB study is not very easy for me. Not only in learning, but also encountered many difficulties in life. However, with the help of teachers and friends, I still overcome the difficulties.

I am sincerely grateful to Professor Martinez Garcia Javier, who teaches me very patiently. Without his supervision and enthusiasm, the production of thesis would not have been possible. Moreover, based on my research, he recommended me a doctoral tutor in UPC. I really appreciate him.

I would also like to express thanks to Professor Manel and teachers from Ningbo University. They established the exchange program to support me to study in

Universitat Politècnica de Catalunya and back home.

In addition, every teacher in the class helped me a lot. They taught me the ability to solve problems independently and the importance of academic integrity.

Finally, I would like to express my gratitude to my family and friends, who have supported me and helped me reach where I am today.

CONTENTS

1.Introduction.....1
1.1 Research background.....1
1.2 Research status of cable force identification of stay cable.....4
1.2.1 Research status of vibration method.....5
1.2.2 Research status of time-varying cable force.....8
1.3 Research content.....8
2. Variational modal decomposition characteristics analysis.....9
2.1 Basic principles of variational mode decomposition.....10
2.2 Simulation signal analysis.....13
2.2.1 Type one modal aliasing.....13
2.2.2 Type two modal aliasing.....16
2.2.3 Noise robustness.....错误！未定义书签。
2.3 Measured signal verification.....22
3. Variational modal decomposition based on parameter optimization.....25
3.1 Particle swarm optimization algorithm.....26
3.1.1 Basic principles of PSO algorithm.....26
3.1.2 PSO algorithm mathematical description.....27
3.1.3 PSO algorithm control variable analysis.....29
3.2 Combining algorithms.....32
3.3 Simulation signal verification.....36
3.4 Measured signal verification.....36
4. Time-varying cable force identification and cable model test.....40
4.1 Hilbert transform and instantaneous frequency.....26
4.2 Processing and Analysis of End Effect of Instantaneous Frequency Curve.....42

4.3 Cable model test..... 43
4.3.1 Test plan design..... 43
4.3.2 Cable force identification result..... 45
5.The application prospect of PSO-VMD time-frequency analysis method in marine engineering..... 49
5.1 Offshore platform vibration monitoring..... 50
5.2 Barge mooring rope load measurement..... 51
6. Conclusion..... 51
Reference..... 52

1.Introduction

1.1 Background

After entering the 20th century, there are countless large-span and super-span structures, public civil buildings, landmark buildings and large bridges built in China. Among various types of structures, bridge structures play an irreplaceable and important role in people's daily lives and for the economic development of the region and the entire country. As of 2008, in according to the official announcement of the Ministry of Communications, the total number of bridges that have been built in China reached 500,000. Moreover, the number continues to grow rapidly. According to statistics, more than 10,000 bridges across the country begin construction every year. For large-span bridge structures, China is far away from the scale and quantity of construction leading the rest of the world, China is also the country with the most types of bridge structures. China's bridge construction is attracting worldwide attention. Its number, scale and short construction period are unprecedented in other countries. Among them, there are more than 1,000 large-scale structures with a total bridge length of more than 1,000 meters. These large-span and super-span bridges are world-class in terms of material selection, structural design, construction and quality acceptance after completion. For example, the Hangzhou Bay Bridge that was opened in 2007 has created many Record. All these indicate that China is steadily moving forward from a "bridge power" and will eventually become a "bridge power" in the world.

At the end of the 20th century, rapid economic development pushed all types of large-span and even super-span bridges to a construction climax. Long-span bridges

have very rich structural forms, ranging from well-known arch bridges with a long history to some new structures and hybrid systems developed in recent years. Among the many structural forms mentioned above, the mainstream choices for long-span bridges are suspension systems and cable-stayed systems. Cable-stayed bridges are also the most rapidly developed and most significant long-span bridges in the past 20 years.

To a certain extent, a bridge is an indispensable part of a road. It serves as a transportation hub to connect roads so that traffic is no longer affected by the obstacles of mountains and rivers. Compared with ordinary public civil buildings, the importance of bridges is often higher, the construction investment is huge and the design life is longer, so the requirements for its basic performance are relatively high. In the entire process from the initial construction of the bridge to the completion of the bridge, the service environment is generally harsh, which results in the serious erosion of the building materials by the harmful substances in the external environment, which eventually leads to the degradation of the material performance. In addition, the bridge has been subjected to long-term dynamic loads such as vehicles and wind, resulting in severe cumulative fatigue damage[1,2]. Due to the combined effects of the above factors, many bridge structures have suffered serious damage or even collapsed before reaching the designed service life. Some bridges have deteriorated to varying degrees in the years after they were built, seriously affecting their function.In recent years, China Bridge The frequent occurrence of the Liang collapse accident has also aroused great attention and attention from the relevant state departments and ordinary people. Figure 1-1 is an example of a bridge collapse accident in recent years. The occurrence of these accidents is related to many factors, but lack of effective monitoring after completion and operation, regular maintenance and repair is undoubtedly one of the important reasons. A large

number of bridge structure monitoring data shows that although there are many bridges in China, the weight and flow of vehicle loads on these bridges far exceed the maximum limits specified in the bridge design specifications. Overweight vehicles have also become recognized "Bridge Killer".

a) Linzhi Bomi Tongmai Bridge

b) Harbin Yangmingtan Bridge

c) Fujian Wuyishan Mansion Bridge

d) Jilin Jinjiang Bridge

Figure 1-1 Bridge collapse accident in recent years

In summary, it is very important for the safety assessment of the bridge structure during the operation period and the regular maintenance based on it after it is built and cannot be ignored. For the cable-stayed bridge, the cable is a very important and

critical component. As we all know, fatigue damage is one of the most complicated and difficult to solve problems in the field of structural engineering. However, cumulative fatigue damage is precisely the main factor that causes bridge damage. During the period when the cable-stayed bridge is put into use, under the combined action of vehicle load traffic and external environment such as wind load, the cable is subjected to various vibrations. The cable force changes in real time. Serious fatigue damage. Therefore, the accurate identification of the real-time changing cable force is the basis for the safety assessment of the limit state of the cable stay and the cumulative fatigue damage assessment. For the entire bridge structure, it has very important reality not only during the construction period but also during the maintenance period Significance[3]. Based on the above importance, the cable force identification in cable-stayed bridges has been a hotspot and focus in related fields at home and abroad for many years[4,5].

1.2 Research status of cable force identification of stay cable

The identification and estimation of cable force are of great practical significance for the maintenance and safety assessment of long-span and super-long-span cable-stayed bridges. Many experts and scholars at home and abroad have conducted research on cable force identification. The existing cable force identification methods include: static method, that is, the tensile force in the cable is directly measured by a hydraulic jack and other force measuring devices; vibration method, that is, indirect cable force identification is performed by measuring the natural frequency of the cable's vibration. In actual applications, traditional force sensors and electromagnetic (EM) sensors are used for direct measurement. Traditional force sensors are used in series with cables, and strain can be measured by vibrating wire sensors, strain gauges, hydraulic sensors, or fiber

Bragg grating sensors. Series connection means that these sensors are not easy to replace and are difficult to calibrate under high stress conditions that occur in field applications. In addition, they often have unstable long-term performance. Therefore, these sensors are not widely used for long-term monitoring of bridge cables. Vibration method has gained wide attention because of its advantages such as simplicity, speed and efficiency.

1.2.1 Research status of vibration method

Vibration - based methods for estimating cable tension forces use a relation between the natural frequency of the cable vibrations and the tension force in the cable. These nondestructive monitoring methods are widely studied and often are used in practice with the advantages of being inexpensive and convenient to install. The existing vibration - based estimation methods can be classified into four categories depending on what cable vibration theory they use[6].

The first category of estimation methods utilizes the flat taut string theory that neglects both sag-extensibility and bending stiffness

$$F = 4mL^2{f_1}^2 \quad (1)$$

where F is the cable tension forces; f_1 is the fundamental natural frequency; and m and L are the mass density and length of cable, respectively. Casas [7] used Eqn 1 to measure cable tension forces in the Alamillo Bridge with accelerometers installed on cables. Gentile [8] used microwave remote sensing to measure the vibration response in the longer cables of two cable - stayed bridges and then

predicted the cable tensions from natural frequencies using the formula as Eqn 1. Kim and Shin [9] have made a comparative study of several tension estimation methods for cable supported bridges and they concluded that taut string theory is a good tool for a first approximation because of its simplicity and quick calculation. Ren et al. [10] discussed the effects of sag and the bending moment on the fundamental frequencies of cables under ambient excitation and concluded that these frequencies are close to the fundamental frequency of a taut-string even when the cable sag and bending stiffness effects are taken into account. Then they used these frequency differences to replace the fundamental frequency in the taut string theory formula and estimated the cable tension forces in laboratory tests and in a field test for the stay cables from the Qingzhou Bridge in China.

For the second category of estimation methods, sag-extensibility is considered but bending stiffness is ignored. Based on this theory, Russell and Lardner [11] experimentally investigated estimation of cable tension forces. On their approach, additional information consisting of the unstrained length of the cable is needed and a nonlinear characteristic equation is solved by trial and error [11]. However, the unstrained length is often not available in practice [6].

For the third category of estimation methods, an axially loaded beam considering bending stiffness but not sag-extensibility is used [12].

$$F = 4mL^2(\frac{f_n}{n})^2 - \frac{EI}{L^2}(n\pi)^2 \qquad (2)$$

where f_n is the nth modal frequency, and EI denotes the flexural rigidity of cable. However, Eqn 2 may cause errors for short and stout cables because this formula is derived from an axially tensioned beam with hinged end boundaries rather

than a fixed one [13]. Fang and Wang [13]proposed a curve-fitting technique to solve the free vibration equation of the cable with two fixed ends, which gave an explicit formula for cable tension estimation, and they then verified their formula with available experimental results and finite element solutions. Sim et al. [14] developed a wireless cable tension monitoring system using MEMSIC's Imote2 (Intel Corporation, Santa Clara, CA, USA) smart sensors, in which Eqn 2 is implemented on the sensors.

The last category of estimation methods takes account of both sag-extensibility and bending stiffness using a practical formula. Zui et al. [15]developed a set of such formulas that were deduced from the cable's free vibration with some assumptions for simplicity. Kim and Park [6] proposed an approach to estimate cable tension force from measured natural frequencies, while simultaneously identifying flexural and axial rigidities of a cable system. They use a finite element model that considers both sag-extensibility and flexural rigidities and then a frequency-based sensitivity-updating algorithm is applied to identify the model. Liao et al. [16]developed a model-based method to simultaneously identify cable tension and other structural parameters from the identified modal frequencies by using a finite element model of the cables combined with a least-squares optimization scheme. Cho et al. [17] embedded the cable tension force estimation equations proposed by Zui et al. [15] into wireless sensors to produce an automated cable tension force monitoring system for cable-stayed bridges.

1.2.2 Research status of time-varying cable force

All of these vibration-based methods are usually not able to estimate the time-varying cable tension forces, but only their average values. In contrast, Li et al. [18] proposed an extended Kalman filter based method to estimate the time-varying cable tension force using the measured acceleration data, but it also needs wind speed data from the bridge. Yang et al. [19] proposed a method to identify time-varying cable tension forces from acceleration data via an unsupervised learning algorithm called complexity pursuit. The method is based on flat taut string theory and tracks the time-varying cable frequency using data from two accelerometers on a cable. Yue et al.[20] proposed a method for identifying bridge time-varying cable forces based on an adaptive sparse time-frequency analysis method. It estimates the instantaneous frequency by looking for the most sparse time-frequency representation of the signal in the largest possible time-frequency dictionary, and then calculates the instantaneous cable force.

1.3 Research content

The thesis studies the identification method of bridge cable time-varying cable force based on variational mode decomposition. Specific research contents include:

(1) Study novel variational mode decomposition (VMD) methods and compare them with existing decomposition models (such as empirical mode decomposition (EMD)). The difference between the two types of modal aliasing problem and noise robustness problem is dealt with by comparing simulated signals with variational mode decomposition and empirical mode decomposition. Finally, the feasibility of

identifying the time-varying frequency by variational modal decomposition is verified on the engineering data.

(2) The effect of VMD processing is seriously affected by the penalty factor and the number of components. It is difficult to set these two parameters at the same time through subjective experience. To solve this problem, the powerful global optimization ability of the particle swarm optimization algorithm is utilized, and the parameters that affect the VMD are searched in parallel. A time-frequency analysis method based on parameter optimization variational modal decomposition is proposed. Through simulation signals and engineering The acceleration signal is verified.

(3) Based on the time-frequency analysis method of parameter-optimized variational modal decomposition, a new time-varying cable force method is proposed. First, the variational modal decomposition method is optimized according to the parameters, the measured cable acceleration signal is decomposed into several sub-signals, and then the time-varying modal frequency of the cable is identified according to Hilbert transform. Then, the cable force is identified based on the relationship between the cable force and frequency established by the classical string vibration theory. The frequency doubling relationship existing in the vibration of the cable is used to reduce the method optimization variables, improve the calculation efficiency, reduce the influence of noise on the different instantaneous frequencies of the cable, and improve the recognition accuracy of the time-varying modal frequency. Finally, the time-frequency relationship of the identified cable is substituted into the cable force formula to obtain the time-varying cable force of the cable. For the end effect of the instantaneous frequency curve, the method of signal extension is used to reduce the error of the instantaneous frequency at the end point. And through the

design and construction of horizontal cable vibration test platform, the results of this paper and test results are compared to further verify the correctness of this method.

2. Variational modal decomposition characteristics analysis

Empirical Mode Decomposition (EMD) [21] is an adaptive signal processing method proposed by Academician Huang E of NASA, which can decompose complex non-stationary nonlinear signals into several eigenmode functions (Intrinsic Mode Function, IMF) component, which has been widely used in the field of mechanical fault diagnosis, but the EMD method lacks a strict mathematical theoretical basis, there is a large amount of iterative calculation, inappropriate envelope fitting, end effect and modal aliasing Wait for a series of problems [22] . In 2014, scholar Konstantin Dragomiretskiy creatively proposed a novel adaptive signal processing method-Variational Mode Decomposition [23] (VMD). VMD is completely different from the recursive decomposition algorithm of EMD. Its overall framework is a constrained variational problem. The VMD algorithm assumes that each modal component is closely centered around a certain center frequency, and transforms the process of determining the modal bandwidth into a constrained variational problem, and realizes the separation of each modal component by solving it. Reasonable adjustment of the parameters of the VMD algorithm can achieve flexible segmentation of the signal frequency domain, thereby effectively mining potential feature information in the signal. Through simulation signals, the difference between VMD and EMD in dealing with two types of modal aliasing problems is compared, and the equivalent filtering characteristics of VMD and EMD are compared using numerical simulation of fractional Gaussian noise. Finally, the feasibility of VMD for engineering data is further discussed.

2.1 Basic principles of variational mode decomposition

In the VMD method, ‘modality’ is redefined as an AM-FM signal, and its

expression is[23] :

$$u_k(t) = A_k(t)\cos\quad(\varphi_k(t))$$

(2-1)

Among them, $\varphi_k(t)$ is the phase of the signal, $A_k(t)$ represents the instantaneous amplitude, $w_k(t) = \varphi_k^{'}(t) = \frac{d\varphi_k(t)}{dt}$ represents the instantaneous frequency, and the phase is in phase In contrast, the instantaneous amplitude and instantaneous frequency are all slow variables.

The VMD method can decompose a real signal into a predetermined number of quasi-orthogonal sub-modes, each of which has a frequency center and a limited bandwidth. In order to distinguish it from the Intrinsic Mode Function (IMF) in the EMD method, this paper refers to the 'modal' component in the VMD method as the Band-Limited Intrinsic Mode Function (BIMF). When acquiring signal components, the VMD method completely abandons the circular recursive screening method adopted by the EMD method, and uniquely transfers it to the variational framework. The signal decomposition process is completed by constructing and solving the constrained variational model, so this method has a solid theoretical foundation. The corresponding constrained variational model can be described as seeking k BIMF components $u_k(t)$ with specific sparsity, so that the sum of the estimated bandwidths of each component is the smallest, and the constraint condition is that the sum of the components is equal to the original signal $f(t)$ The specific construction steps of the model are as follows:

(1) Through Hilbert transform, the analytical signal of each BIMF component $u_k(t)$ is obtained, the purpose is to obtain its unilateral frequency spectrum:

$$\left(\delta(t) + \frac{j}{\pi t}\right) * u_k(t) \qquad (2\text{-}2)$$

(2) For the analytical signal of each BIMF component, estimate the corresponding center frequency ω_k, multiply it with the exponential signal$e^{-i\omega_k t}$, and move the spectrum to the base band:

$$\left[\left(\delta(t)+\frac{j}{\pi t}\right)*\mathrm{u_k}(t)\right]e^{-i\omega_k t} \tag{2-3}$$

(3) Calculate the square of the 2L norm of the above modulation signal gradient, estimate the bandwidth of each BIMF component, and finally construct a constrained variation model of the following form:

$$\begin{cases}\min\limits_{\{\mathrm{u_k}\},\{\omega_k\}}\sum_{k=1}^{K}\left\|\partial_t\left[\left(\delta(t)+\frac{j}{\pi t}\right)*\mathrm{u_k}(t)\right]e^{-i\omega_k t}\right\|_2^2 \\ s.t.\sum_{k=1}^{K}\mathrm{u_k}(t)=f(t)\end{cases} \tag{2-4}$$

Where $\delta(t)$ is the unit pulse function, j is the imaginary unit, * represents the convolution operation, ∂_t represents the partial derivative of the function, $\{u_k\}=\{u_1,u_2,\ldots,u_K\}$ represents the K BIMF component, $\{w_k\}=\{w_1,w_2,\ldots,w_K\}$ represents the center frequency of each component.

In order to solve the above variational problem, a penalty factor α and a Lagrangian multiplier λ are introduced to turn the constrained variational problem into an unconstrained variational problem, and an augmented Lagrangian expression of the following form is obtained

$$\begin{aligned}L(\{\mathrm{u_k}\},\{\mathrm{w_k}\},\lambda) &= \alpha\sum_{k=1}^{K}\left\|\partial_t\left[\left(\delta(t)+\frac{j}{\pi t}\right)*\mathrm{u_k}(t)\right]e^{-i\omega_k t}\right\|_2^2 \\ &+\left\|f(t)-\sum_{k=1}^{K}\mathrm{u_k}(t)\right\|_2^2+\langle\lambda(t),f(t)-\sum_{k=1}^{K}\mathrm{u_k}(t)\rangle\end{aligned} \tag{2-5}$$

Use the Alternate Direction Method of Multipliers (ADMM) to iteratively update u_k^{n+1}, w_k^{n+1}, and λ^{n+1} and search for Saddle point in formula (2-5), then complete the constrained variational question in formula (2-4). During the search for 'saddle point', the corresponding variable update expression is as follows:

$$\dot{u}_k^{n+1}(\omega) = \frac{\dot{f}(\omega) - \sum_{i=1}^{k-1} \dot{u}_i^{n+1}(\omega) - \sum_{i=k+1}^{k} \dot{u}_i^{n}(\omega) + \frac{\dot{\lambda}^n(\omega)}{2}}{1 + 2\alpha\left(\omega - \omega_k^n\right)^2} \tag{2-6}$$

$$\omega_k^{n+1} = \frac{\int_0^\infty \omega \left|\dot{u}_k^{n+1}(\omega)\right|^2 d\omega}{\int_0^\infty \left|\dot{u}_k^{n+1}(\omega)\right|^2 d\omega} \tag{2-7}$$

$$\lambda^{n+1}(\omega) = \lambda^n(\omega) + \tau\left(\dot{f}(\omega) - \dot{u}_k^{n+1}(\omega)\right) \tag{2-8}$$

'.' Represents the Fourier transform, and n is the number of iterations. τ is the fidelity coefficient.

In the process of iteratively solving the variational model, the frequency center and bandwidth of each BIMF component are continuously updated until the iteration stop condition $\sum_{k=1}^{K}\left(\left\|\dot{u}_k^{n+1}(\omega) - \dot{u}_k^{n}(\omega)\right\|_2^2 / \left\|\dot{u}_k^{n}(\omega)\right\|_2^2\right) < \varepsilon$, end the whole loop, and finally complete the adaptive segmentation of the signal band according to the frequency domain characteristics of the actual signal, and pass The inverse Fourier transform transforms the resulting $\{\dot{u}_k(\omega)\}$ into the BIMF component in the time domain.

2.2 Simulation signal analysis

Huang et al. Discovered modal aliasing when studying EMD processing intermittent signals[24] . Zhao Jinping pointed out through further research that intermittent interference, accidental pulses and noise caused abnormal events such as signal incoherence that caused modal aliasing in EMD [25]. The specific appearance of modal aliasing is that the same modal component has different feature time scales, or the similar feature time scales are distributed in different modal components, which causes the adjacent two modal components to interfere with each other, and the feature mixing cannot be distinguished. In this paper, modal aliasing is divided into two categories. The first category is modal aliasing caused by vents,

n=n+1

and the second category is modal aliasing caused by modal component frequencies being too close. In this section, the simulation and comparative study of VMD and EMD is conducted to verify the advantages of VMD in dealing with two types of modal aliasing problems.

2.2.1 Type one modal aliasing

In order to simulate intermittent signal interference, two low-frequency signals and intermittent high-frequency signals are used to synthesize the simulated signal $x(t)$. a cosine signal $x_1(t) = 0.5\cos(360\pi t)$ with a duration of 0.1s is added to the cosine signal $x_2(t) = 1.2\cos(24\pi t)$ and cosine signal $x_3(t) = 0.6\cos(140\pi t)$ every 0.2s.The set sampling frequency is 1000Hz, and the number of analysis points is 1000 points. The time-domain waveform of the intermittent synthesized signal x (t) and its components is shown in Figure 2-2, and the corresponding formula is as follows:

$$x(t) = x_1(t) + x_2(t) + x_3(t) \tag{2-9}$$

EMD processing of this signal, the results shown in Figure 2-3. EMD divides the synthesized signal adaptively. The solution was 7 IMF components, and there was over-decomposition. 180Hz high frequency is mixed in the IMF1 component. The discontinuous cosine component and the 70 Hz cosine component, the signal characteristics are aliased and cannot be resolved, and a large degree of distortion occurs. The IMF3 component is the separated 12Hz cosine component, while IMF2, IMF4, IMF5, IMF6, and IMF7 are false components due to modal aliasing. In the process of EMD signal processing, there is an error between the actual signal envelope curve and the mean curve and the theoretical value, and the error produces a cumulative effect through successive iterative operations, which eventually leads to the occurrence of modal cracking and aliasing.

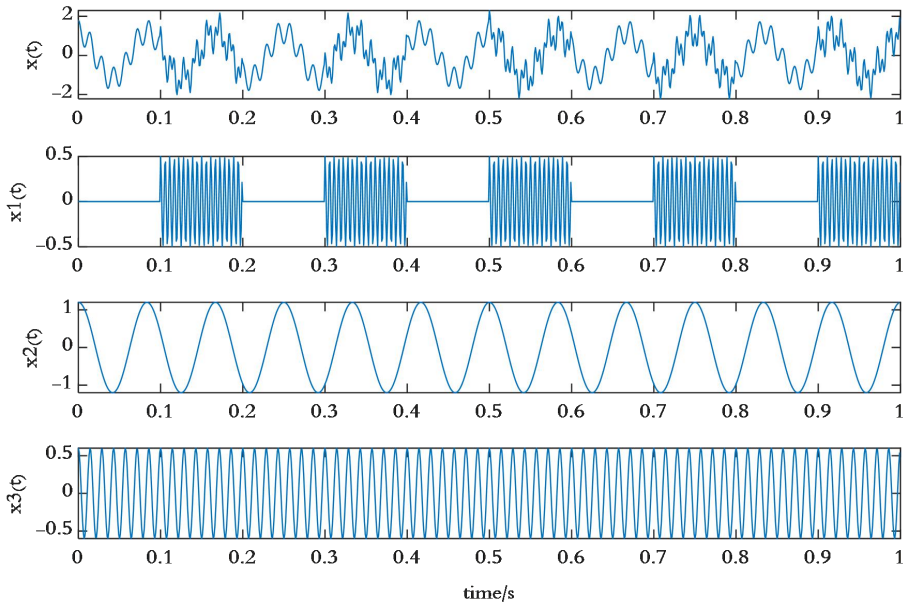

Fig.2-2 Waveforms of composite interruption signal and its components

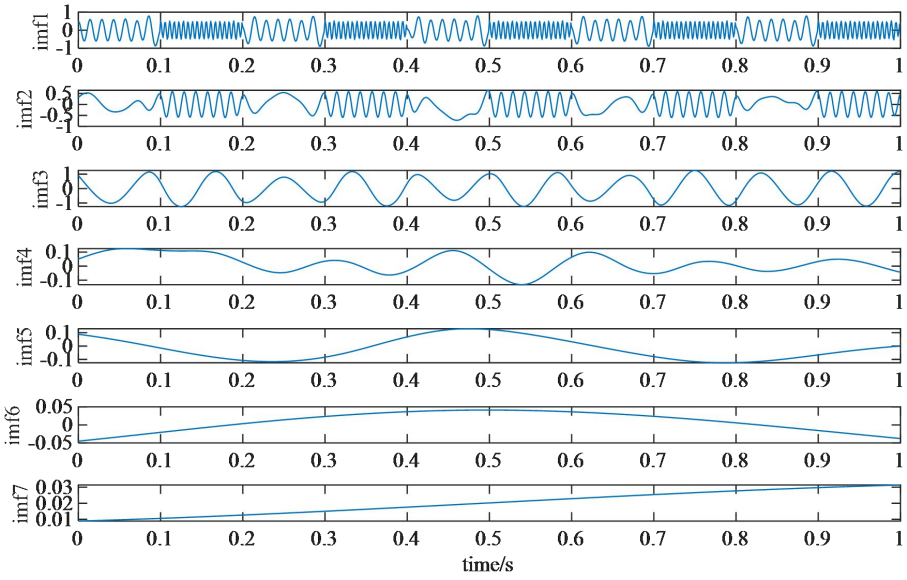

Fig.2-3 Processing results of EMD for composite interruption signal

Perform VMD processing on the above intermittent synthesized signal, set the

penalty factor $\alpha = 300$, and the number of components K = 3. Observing the processing results, you can find that the 180Hz discontinuous high-frequency component and 70Hz.

The 12Hz low-frequency components are successfully stripped away, and the position of the middle high-frequency cosine component of the BIMF3 component. And the duration is basically consistent with the $x_1(t)$ component, except for slight reconstruction errors on both sides of the signal mutation position. The BIMF1 and BIMF2 components more accurately restore the original characteristics of the $x_2(t)$ and $x_3(t)$ components. The processing effect is significantly better than the EMD method. Because the VMD method obtains signal components through a specific variational model solution method, it can suppress the adverse effects caused by abnormal interference factors in the process of recursive screening and stripping operations, thereby effectively avoiding the first type of modalities that occur in the process of EMD processing signals The aliasing problem.

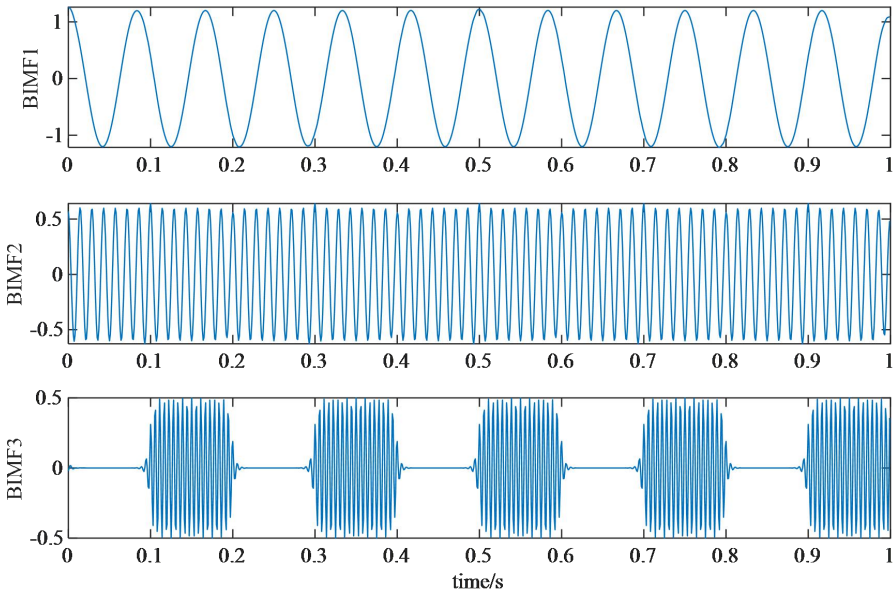

Fig.2-4 Processing results of VMD for composite interruption signal

2.2.2 Type two modal aliasing

EMD also has another aliasing phenomenon caused by the frequency of the modal components being too close. Literature [26] pointed out that in the process of EMD signal processing, when the frequency f_h of the high frequency component and the frequency f_l of the low frequency component satisfy $f_l/f_h > 0.67$. That is, when the frequencies of the two components are too close, no matter what the amplitude ratio of the signal is, EMD cannot separate them correctly. The following uses a set of three simulated frequency signals of similar synthesized signals $x(t)$ for analysis, where the 38Hz high frequency signal is $x_1(t) = \cos(76\pi t)$, the 32Hz intermediate frequency signal is $x_2(t) = \cos(64\pi t)$, 20Hz low-frequency signal is $x_3(t) = \cos(40\pi t)$, the set sampling frequency is 1000Hz, the number of analysis points is 1000 points, and the time-domain waveform of the near-frequency synthesized signal and its components is shown in Figure 2-5. The expression is as follows:

$$x(t) = x_1(t) + x_2(t) + x_3(t) \tag{2-10}$$

EMD processing the above signals, the results are shown in Figure 2-6. It can be seen from this that EMD adaptively decomposes the synthesized signal into three IMF components. The IMF1 component waveform is close to the original signal, which contains 38Hz high frequency, 34Hz intermediate frequency and 20Hz low frequency components. IMF2 and IMF3 are the false components generated by the cumulative effect of EMD continuous iterative operation errors. The components in the original signal are too dependent on the frequency. Recently, it cannot be resolved, and modal aliasing has occurred.

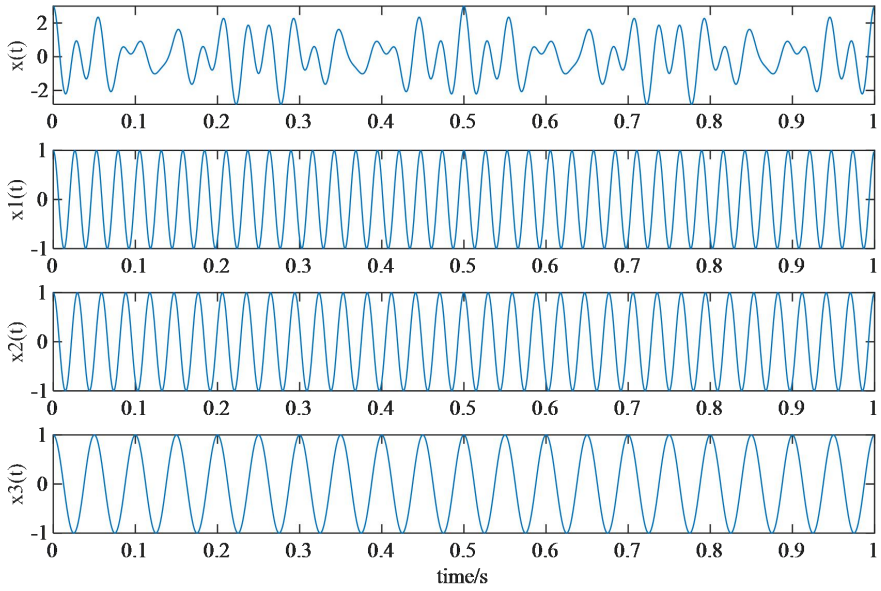

Fig.2-5 Waveforms of composite close-frequency signal and its components

Using VMD to process the above-mentioned near-frequency synthesized signal, set the penalty factor = 300, the number of components K = 3, the processing results shown in Figure 2-7. VMD decomposes the original signal from high frequency to low frequency into three BIMF components. The 38Hz, 34Hz, and 20Hz cosine components of the original signal are successfully separated. Observing the endpoints of BIMF1 ~ BIMF3, it is not difficult to find that there is a slight degree of 'distortion' in the amplitude and phase of the two ends, mainly due to the endpoint effect of VMD, but compared to the recursive modal decomposition method of EMD, the endpoint of VMD The effect is weak and will not propagate into the signal as the number of loop iterations increases. From the perspective of signal processing effect, compared with the EMD method, the VMD method can more accurately separate the components of the original near-frequency synthesized signal, and can effectively solve the second type of modal aliasing caused by the close frequency of the signal components.

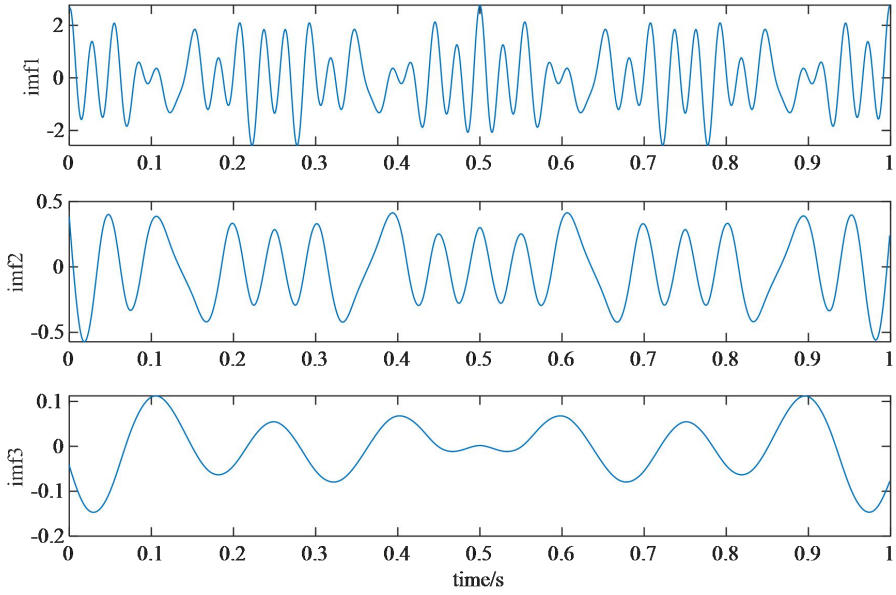

Fig.2-6 Processing results of EMD for composite close-frequency signal

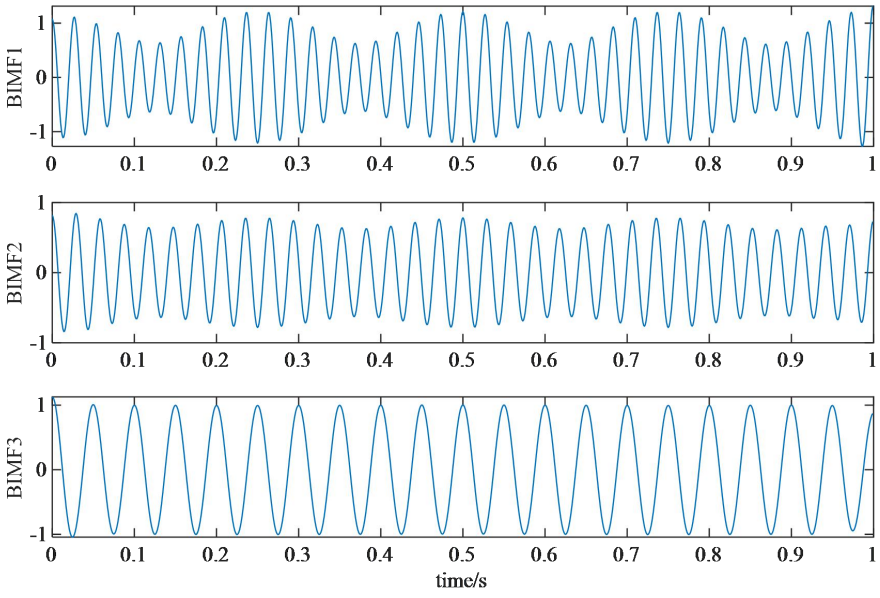

Fig.2-7 Processing results of VMD for composite close-frequency signal

2.2.3 Noise robustness

To illustrate the robustness of VMD with respect to noise in the input signal, we use the following three-harmonic signal with entrained noise for testing:

$$f_n(t) = \cos(4\pi t) + \frac{1}{4}\cos(48\pi t) + \frac{1}{16}\cos(576\pi t) + \eta \qquad (2\text{-}11)$$

Where η ~ ñ (0, σ) represents Gaussian noise, and σ represents the control noise level (standard deviation). Here we choose σ = 0.1, which is very important for the amplitude of the highest and weakest harmonics. We decompose the variational mode into three modes without the Lagrange multiplier to eliminate noise. Figures 2-9 show the signal and the three components estimated using VMD. The low-frequency high-amplitude signal can be almost perfectly recovered, and the recovery of the intermediate-frequency mid-amplitude signal is also acceptable, but it is not easy to obtain the high-frequency low-amplitude signal. The VMD algorithm can correctly adjust the third center frequency on this harmonic, but the recovery mode will be severely affected by noise. Here, the risk of reducing the bandwidth α by increasing the bandwidth is that the correct center frequency cannot be captured correctly, and a too low α contains more noise in the estimation mode. However, this pattern can be further cleared in post-processing.

Figure 2-10 shows that the exact same signal is processed using EMD, which generates 7 estimation modes. The first two modes contain the highest frequency harmonics and a lot of noise. The third mode is closest to the mid-harmonic, but important features have been attributed to the fourth and fifth modes. The sixth mode absorbs most of the low-frequency harmonics, but is severely distorted.

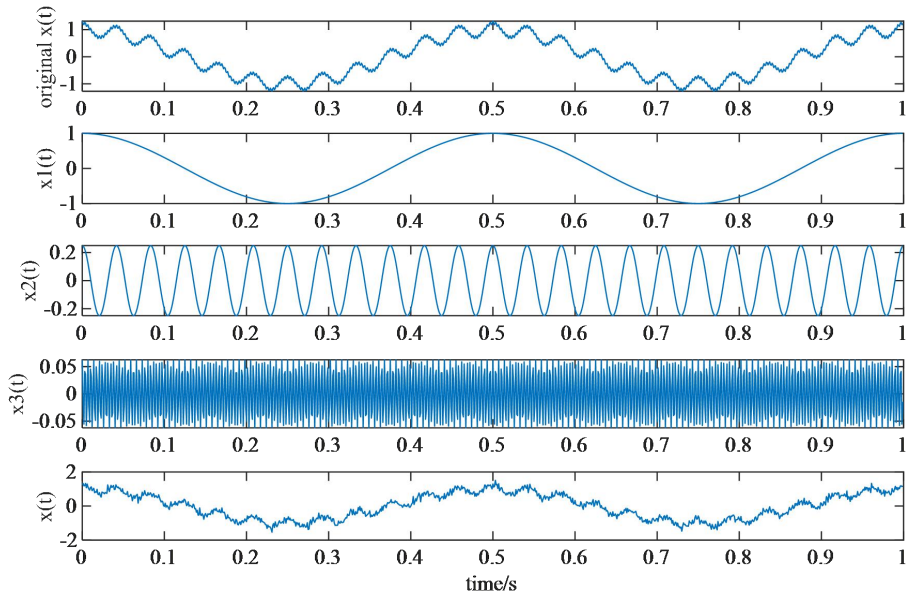

Fig.2-8 Three-harmonic signal and its component waveform

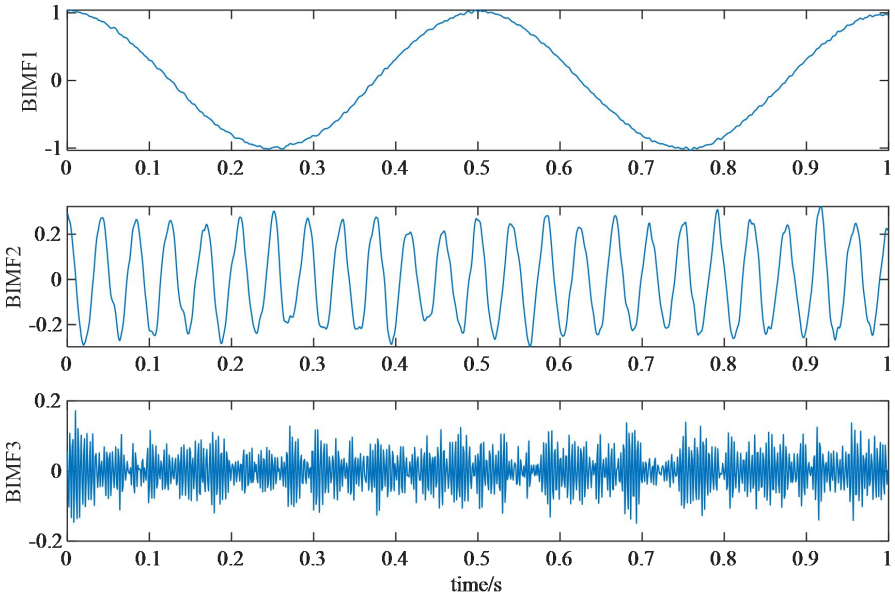

Fig.2-9 Processing results of VMD for Three-harmonic signal

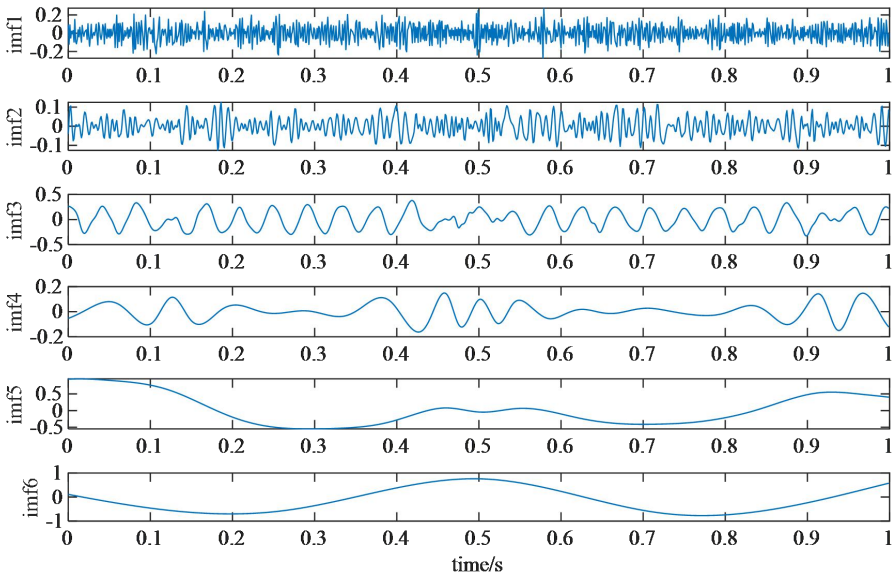

Fig.2-10 Processing results of EMD for Three-harmonic signal

2.3 Measured signal verification

In order to better verify the reliability of the modal decomposition of VMD, the acceleration signal of a bridge cable in the project is used for testing. The sampling frequency is 50 Hz, and the number of analysis points is 6000 points. The acceleration time history chart and spectrum chart are shown in Figure 2-11 below. It can be seen from the figure that the first few order modes of the tested cable are excited, the fundamental frequency of the cable is around 1.34 Hz, and the frequency doubling relationship between the frequencies corresponding to each order mode is also very obvious.

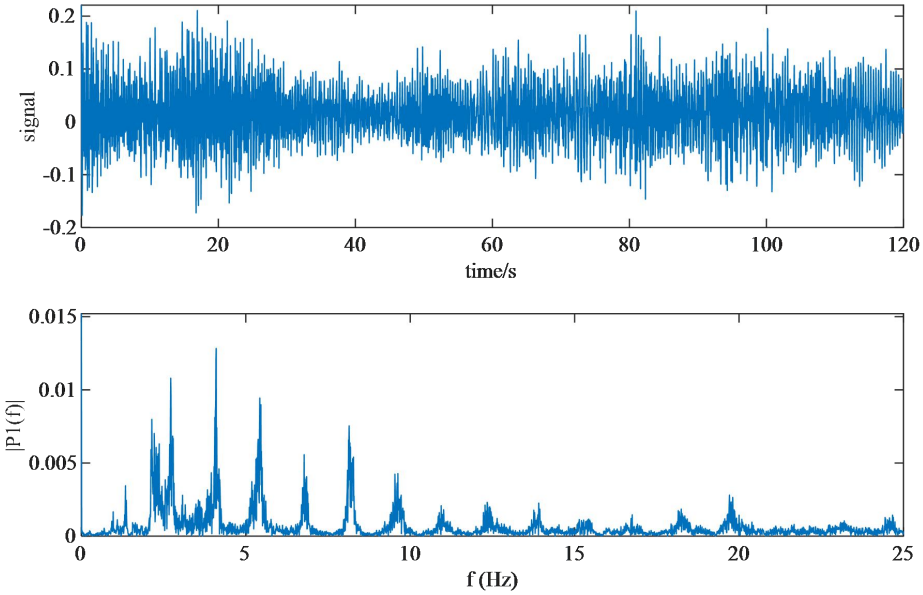

Fig.2-11 Acceleration time history chart and spectrogram

According to the spectrogram of the cable acceleration signal, it is inferred that the decomposition order is about 14 orders. Therefore, set the number of components of the VMD algorithm K = 14, and the penalty factor α is set to 600 according to experience. Figure 2-12 is the result of analyzing the cable acceleration signal. It can be seen that u3 ~ u10 are well separated, and the center frequency is consistent with the 3rd to 10th order frequencies of the original signal. And the noise signal is filtered out and is almost a single signal, which is beneficial to the subsequent Hilbert transform processing.

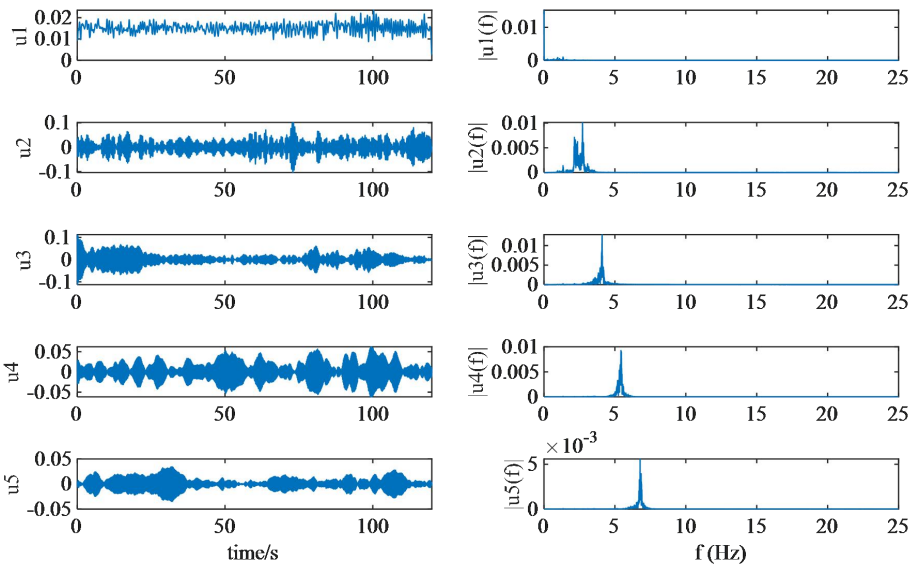

a) Acceleration time-histogram and spectrum diagram of u1, u2, u3, u4, u5

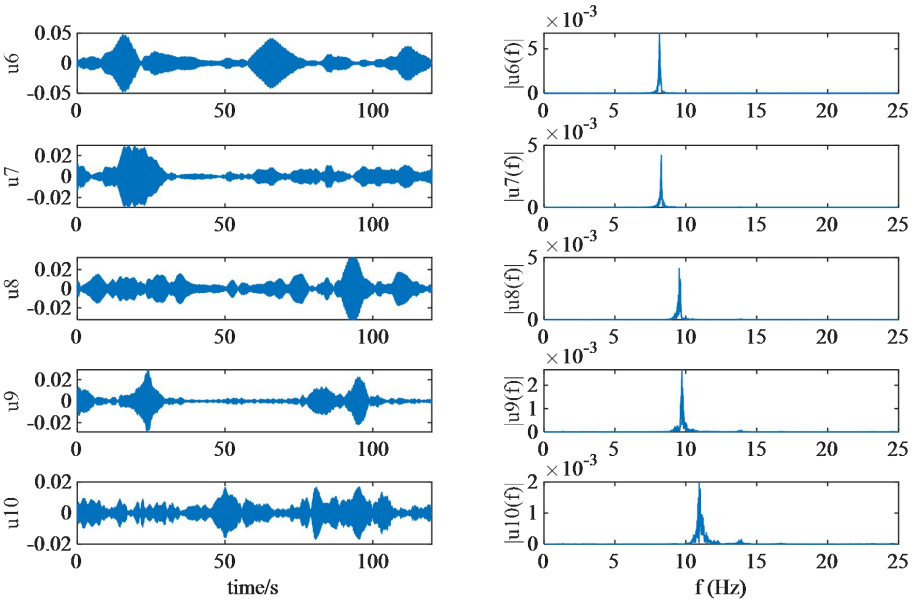

b) Acceleration time-histogram and spectrum diagram of u6, u7, u8, u9, u10

VMD processing

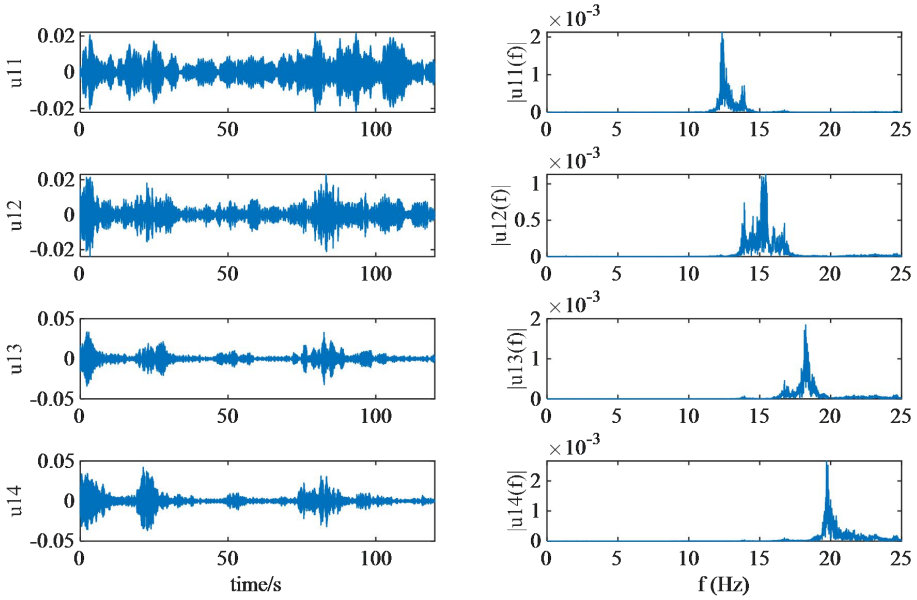

c) Acceleration time-histogram and spectrum diagram of u11, u12, u13, u14

Fig.2-12 Processing results of VMD

This chapter briefly introduces the basic principle and implementation process of VMD, and compares it with EMD through discontinuous synthesized signal and near-frequency synthesized signal. The results show that VMD can separate modes with different center frequencies to a greater extent, which is not only effective It suppresses the modal aliasing caused by signal discontinuity, and successfully solves the modal aliasing caused by the signal frequency being too close, which is obviously superior to the EMD method in avoiding the two types of modal aliasing problems. The numerical simulation of Gaussian noise compares VMD and EMD, and the results show that VMD is more robust. The feasibility of VMD in the processing of cable acceleration data is verified by analyzing the engineering measured signals.

3. Variational modal decomposition based on parameter optimization

In practical engineering applications, the cable vibration signal picked up by the sensor is often mixed with strong background noise, which will affect the accuracy of time-varying cable force identification. Therefore, it is necessary to study reasonable and effective identification methods. In view of the flexible signal frequency domain splitting characteristics of the VMD algorithm, it is tried to analyze the cable force acceleration signal, but the VMD processing effect is seriously affected by the penalty factor and the number of components. It is difficult to set these two parameters simultaneously through subjective experience. To solve this problem, the powerful global optimization ability of the particle swarm optimization algorithm is used, and the parameters that affect the VMD are searched in parallel. A variational modal decomposition method based on parameter optimization is proposed and verified by simulation signals and engineering measured signals.

3.1 Particle swarm optimization algorithm

3.1.1 Basic principles of PSO algorithm

In the mid-1990s, in the process of studying the foraging behavior of bird swarms, American scholar Dr. Russell Eberhart and Dr. James Kennedy were inspired to collaborate and propose an adaptive random optimization algorithm based on population search strategy-Particle Swarm Optimization (Particle Swarm Optimization) , PSO) algorithm[27]. In the PSO algorithm, each particle has a corresponding speed and position, which is used to adjust its own state. The position of each particle represents a potential solution to the problem to be optimized. The PSO algorithm is implemented based on iterative operation. Before the start of the

iteration, the particle population of a preset size is initialized, that is, the initial speed and initial position of each particle are randomly generated. In the subsequent iterative operation process, each particle is calculated and compared Its fitness function value is constantly updated to adjust its own speed and position by tracking its own current best position (local optimal solution) and the entire population's best position (global optimal solution), in a multidimensional space The solution is searched. When the preset maximum population evolution algebra is reached, the whole optimization process is ended, and the goal of approaching the global optimal solution is finally achieved. The PSO algorithm does not need to set too many parameters, and the implementation process is relatively simple. As an efficient search optimization algorithm, it has been widely used in many research fields.

3.1.2 PSO algorithm mathematical description

Suppose that in a D dimensional target search space, there is a particle population composed of m particles, and the position of the i-th particle in the D dimensional space is determined by the vector $X_i = (x_{i1},x_{i2},...,x_{iD})^T$ (That is, the potential solution of the optimization problem), and the velocity of the i-th particle is represented by the vector $V_i = (v_{i1},v_{i2},...,v_{iD})^T$. The best position (local optimal solution) experienced by the i-th particle itself is represented by the vector $P_i = (p_{i1},p_{i2},...,p_{iD})^T$, the best position experienced by the entire population (global optimal solution) Vector $P_g = (p_{g1},p_{g2},...,p_{gD})^T$. In the PSO algorithm, each particle updates its own speed and position according to the following expression[28]:

$$\begin{cases} v_{id}^{k+1} = \omega v_{id}^{k} + c_1\eta\left(p_{id} - x_{id}^{k}\right) + c_2\eta\left(p_{gd} - x_{id}^{k}\right) \\ x_{id}^{k+1} = x_{id}^{k} + v_{id}^{k+1} \end{cases} \tag{3-1}$$

In the formula, i = 1,2, ..., m; d = 1,2, ..., D; k is the current evolutionary algebra; c_1 and c_2 are learning factors; ω is the inertia weight; η is distributed in [0,1] Random number in the range.

It can be found from equation (3-1) that the velocity V^{k+1} of the particle's current evolutionary algebra is obtained by adding three parts of vectors: the velocity V^k of the particle's last evolutionary algebra; the best position experienced by the particle itself The distance from the position of the particle's previous evolutionary algebra $(P_{pbest} - X^k)$; the distance between the best position experienced by the population and the position of the particle's previous evolutionary algebra $(P_{gbest} - X^k)$. The position X^{k+1} of the particle's current evolutionary algebra is obtained by adding the position X^k of the last round of evolutionary algebra to the velocity V^{k+1} vector of the current evolutionary algebra. In the subsequent iteration of the PSO algorithm, each particle continuously updates its own speed and position in this way, and gradually moves closer to the global optimal solution.

3.1.3 PSO algorithm control variable analysis

In order to better understand the PSO algorithm, the main control variables involved include: population size, inertia weight, learning factor, and maximum flight speed [29].

(1) Population size

In the PSO algorithm, the population size M represents the number of particles included. The larger the value of the population size M, the more particles that collaborate with each other, and the stronger the ability of the population to optimize, but at the cost of greater time loss , And the value of M is too small, it will reduce the effective use of global information in the search process, easy to fall into local optimal. Under normal circumstances, the selection of the population size should be based on the actual demand, and the value range of M is generally between [20, 50].

(2) Inertia weight

The inertial weight ω represents the influence of the speed of the last evolutionary algebra of the particles on the current evolutionary algebraic speed. This parameter is an important control variable in the PSO algorithm and can play a

role in balancing the global and local search capabilities of the population. The larger the value of ω, the stronger the global search ability of the population, the weaker the local search ability, and the smaller the value of ω, the opposite effect occurs. The inertial weight ω usually takes a constant value. Generally, when 0.9≤ω≤1.2, the overall search capability of the PSO algorithm is relatively good. Related scholars have found that [30], during the iterative calculation process, ω can be dynamically assigned: at the beginning of the search, a larger value of ω can be assigned to strengthen the global search ability of the population, making it faster in a larger target space Locate the approximate position of the optimal solution. In the late stage of the search phase, continuously reduce the value of ω to strengthen the local search ability of the population, so that the particles can perform detailed search in the area near the extreme point, and drive the particles to the global optimal solution as much as possible 'S position is close.

(3) Learning factor

The learning factor in the PSO algorithm reflects the information sharing and collaboration among particle populations, and c_1 and c_2 affect the ability of particles to learn from their own historical experience and population historical experience, respectively. If the value of the learning factor is too small, the particles may not reach the target area, and only hover outside the area. Otherwise, the particles may quickly move to the target area or even pass through the target area. When $c_1 = 0$ and $c_2 \neq 0$, the particle cannot learn from its own historical experience, only has population experience, it has a fast convergence speed, is easy to fall into a local extremum, and its ability to optimize the complex problem becomes poor. When $c_1 \neq 0$ and $c_2 = 0$, the particles do not have the ability to learn from the historical experience of the population, but only have their own experience. Each particle is like a piece of sand, and the probability of obtaining the global optimal solution is small. In order to make the individual experience and the population experience play the same role and effectiveness, in order to balance, usually set the

learning factor $c_1 = c_2$.

(4) Maximum flight speed

The maximum flight speed V_{max} represents the maximum speed at which particles can move. The larger the value of V_{max}, the stronger the population search ability, but it is easy to skip the optimal solution or even deviate from the solution range. The smaller the value of V_{max}, the easier it is to fall into the local optimal vortex . In order to limit the speed of particles, there is a maximum flight speed limit value in each dimension in the target search space, and the speed of particles is limited to [$-V_{max}$, V_{max}]. The value of V_{max} is generally 10% to 20% of the maximum adjustment step, where the maximum adjustment step refers to the difference between the upper and lower limits of the value of the particle position.

3.2 Combining algorithms

In the process of solving the constrained variational model, in order to convert the constrained variational problem into an unconstrained variational problem, a penalty factor needs to be introduced. This parameter mainly affects the bandwidth of the decomposed BIMF component. The smaller the penalty factor is, the fatter the spectrum is, that is, the bandwidth is larger, and aliasing is easy to occur. On the contrary, the bandwidth is narrower, and modal aliasing is less likely to occur, but the information contained in the BIMF component may be insufficient. Before processing signals with VMD, the number of BIMF components needs to be preset, but there is currently no unified reference standard for the selection of the K value of components [31-33], which basically depends on human subjective experience. The research in Chapter 2 of this paper shows that if the value of K is too small, multiple 'modalities' in the original signal may coexist in the same BIMF component, resulting in some 'modalities' that cannot be effectively identified, resulting in underdecomposition or leak decomposition. If the value of K is too large, a certain 'mode' in the signal may be 'dragged' into multiple BIMF components, resulting in excessive decomposition. The VMD algorithm is simultaneously affected by the

penalty factor α and the number of components K. The reasonableness of these two parameter settings has a crucial impact on the final signal processing results. Therefore, the optimal selection of parameters α and K is to use VMD to diagnose the bearing The key to early failure. If one of the parameters is kept unchanged, only the other parameter is optimized and selected. This local optimization method ignores the interaction between the parameters and obtains only a relatively optimal solution. As an efficient and robust swarm intelligence optimization algorithm, the PSO algorithm has a good global optimization ability. In order to overcome the shortcomings of the subjective selection of VMD key influence parameters, to achieve automatic screening of the penalty factor α and the number of components K, this chapter The PSO algorithm is used to perform parallel search on the influencing parameters of VMD.

When searching for the influence parameters of the VMD algorithm using particle swarm optimization, a fitness function needs to be determined. Each time the particle updates its position, the fitness value is calculated and updated by comparing the new particle fitness value. Shannon entropy is a good standard for evaluating the sparse characteristics of signals. The size of the entropy value reflects the uniformity of the probability distribution. The most uncertain probability distribution (equal probability distribution) has the largest entropy value [34]. In this paper, the concept of envelope entropy is put forward. The envelope signal obtained after the signal demodulation operation is processed into a probability distribution sequence p_j. The entropy value calculated by it reflects the sparse characteristics of the original signal. Zero mean signal. The envelope entropy E_p of $X(j)(j = 1,2,\ldots,N)$ can be expressed as

$$\begin{cases} E_p = -\sum_{j=1}^{N} p_j lg p_j \\ p_j = a(j)/\sum_{j=1}^{N} a(j) \end{cases} \tag{3-2}$$

In the formula, p_j is the normalized form of $a(j)$; $a(j)$ is the envelope signal obtained by Hilbert demodulation of signal $x(j)$.

After the acceleration signal is processed by the VMD algorithm, if the resulting IMF component contains more noise and the frequency doubling characteristic is not obvious, the sparseness of the component signal is weaker and the envelope entropy value is larger. If the IMF component contains more frequency doubling feature information and regular pulses appear in the waveform, the signal will show a stronger sparse characteristic and the envelope entropy value is smaller. When the i-th particle is at a certain position x_i (corresponding to a set of influencing parameter combinations α and K), the envelope entropy values of all IMF components obtained by VMD processing at this position are calculated, and the smallest one It is called the local minimum entropy value, which is expressed by $min_L E_p^{IMF}$. The IMF component corresponding to the local minimum entropy value is the best component that contains frequency doubling information in the group of IMF components. In this paper, the local minimum entropy value is taken as the fitness value in the optimization process, and the minimum local entropy value is minimized as the final optimization goal. The optimization steps of α and K of the VMD algorithm are as follows:

(1) Initialize the parameters of the particle swarm optimization algorithm and determine the fitness function in the optimization process.

(2) Initialize the particle population, use the influence parameter combination $[\alpha,k]$ as the particle position, randomly generate a certain number of influence parameter combinations as the initial position of the particle, and randomly initialize the movement speed of each particle.

(3) Perform VMD calculation on the signal under different particle position conditions to calculate the fitness value corresponding to each particle position $min_L E_p^{IMF}$.

(4) Compare the fitness value and update the individual local extreme value and the population global extreme value.

(5) Use equation (4) to update the particle velocity and position.

(6) Loop iteration, go to step (3), output the best fitness value and particle position after the number of iterations reaches the maximum set value.

3.3 Simulation signal verification

The simulation signal is used to verify the effectiveness of the method in this paper. According to the characteristic that the cable acceleration signal has frequency doubling, the fundamental frequency is set to 8 Hz. The simulation signal is as follows:

$$x(t) = 0.5\cos(2\pi f_1 t) + 0.5\cos(2\pi f_2 t) + 0.5\cos(2\pi f_3 t) + 0.5\cos(2\pi f_4 t) + 0.5\cos(2\pi f_5 t) + \eta \quad (3\text{-}2)$$

In the formula, f_1、f_2、f_3、f_4 and f_5 are equal to 8Hz、16Hz、24Hz、32Hz and 40Hz, respectively. Where $\eta \sim n(0,\sigma)$ represents Gaussian noise, and σ represents the control noise level (standard deviation). Here we choose σ = 0.6.

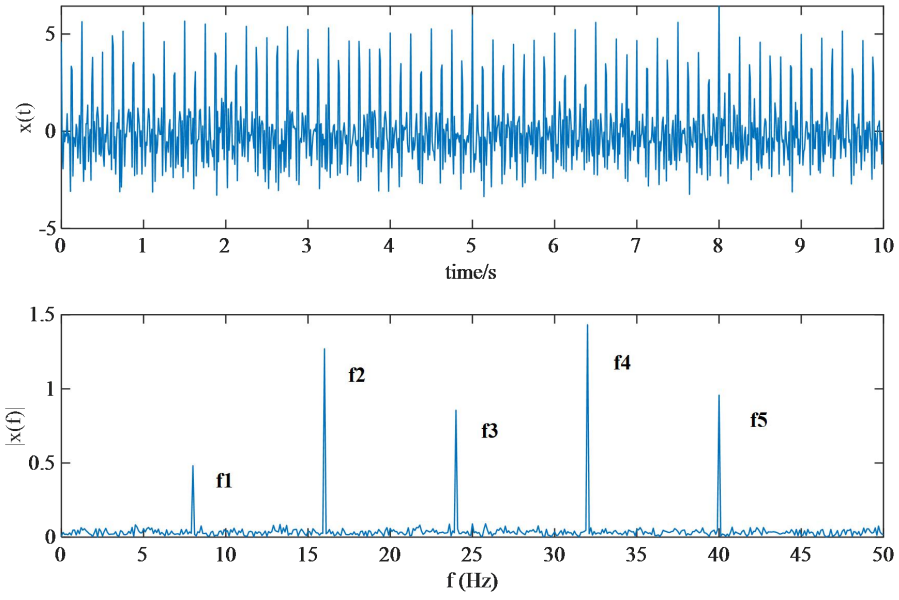

Figure 3-1 Simulation signal waveform and spectrum

Figure 3-1 is the simulation signal waveform and spectrum diagram, from which we can see that the simulation signal frequency shows a frequency-doubling relationship, which is consistent with the assumption. The PSO-VMD analysis results of the simulated signal are shown in Figure 3-2. The variation of the local minimum entropy value with the population evolution algebra in the particle swarm optimization process is shown in Figure a. Obviously, the minimum value of the local minimum entropy value 6.6989 appeared in the ninth generation, and the best influencing parameter combination found $[\alpha_0, K_0] = [425.0926, 6.3458]$, which sets $\alpha = 425$ and K = 6 of the VMD algorithm, and processes the simulation signal. The original signal is processed by the parameter optimization variational modal decomposition algorithm to obtain 6 BIMF signals, and the spectrum diagram is further obtained by FFT. The center frequencies of u_1、u_2、u_4、u_5 and u_6 are 88Hz、16Hz、24Hz、32Hz and 40Hz, which are consistent with f_1、f_2、f_3、f_4 and f_5, indicating that the frequency components of each order are well separated. The center frequency of u_3 is 20Hz and the frequency is mixed, which may be a problem caused by over-decomposition, but it does not affect the subsequent calculation of cable force identification.

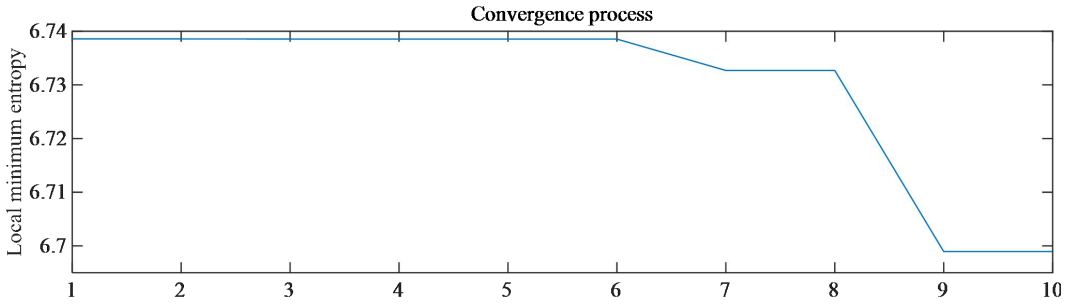

a) The change of local minimum entropy with evolutionary algebra

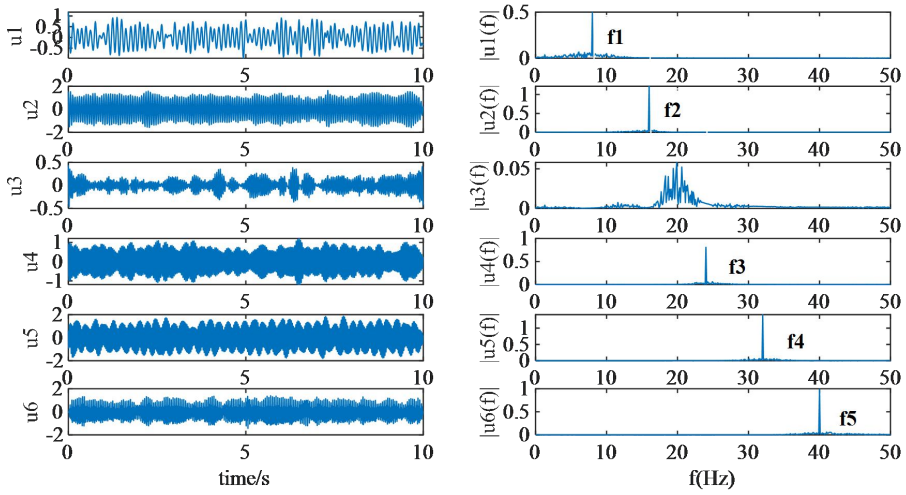

b) Signal waveform and spectrum after VMD processing

Figure 3-2 VMD analysis results of simulated signals

In order to verify the advantages of this method, the EMD algorithm was used to process the above-mentioned simulated signals and do spectrum analysis. Figure 3-3 is the result of EMD processing of the simulation signal, a total of 8 decomposition components $imf_1 \sim imf_8$ are obtained. After comparison, only the first three components $imf_1 \sim imf_3$ have large energy and strong correlation. Among them, the characteristic frequency related components are basically concentrated in the spectrogram of the imf_1 component, and the imf_2 and imf_3 components respectively reflect the third and first order frequency characteristics f_3 and f_1, and the characteristic frequency component is two There is interference frequency on the side, and the background noise is seriously polluted. The energy of the IMF component that is subsequently decomposed is small and related to the original signal. The degree is not large and belongs to the false component lacking actual physical meaning.

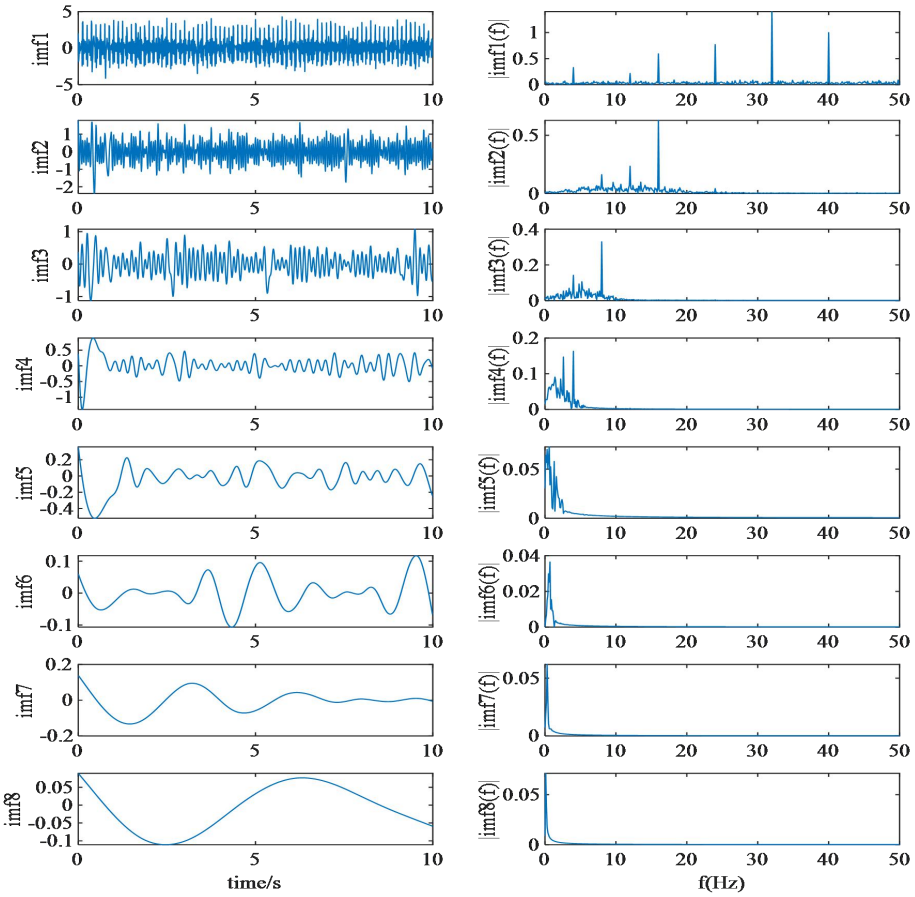

Figure 3-3 EMD analysis results of simulated signals

3.4 Measured signal verification

In order to better verify the reliability of modal decomposition of PSO-VMD, the engineering cable acceleration signal of Chapter 2 is used for testing. The sampling frequency is 50 Hz, and the number of analysis points is 6000 points. The acceleration time history chart and spectrum chart are shown in Figure 3-4 below. It can be seen from the figure that the fundamental frequency of the cable is near 1.34Hz, and the first 14th order frequencies are more obvious, namely 1.324Hz, 2.717Hz, 4.1Hz, 5.458Hz, 6.775Hz, 8.142Hz, 9.625Hz, 10.94Hz, 12.34Hz , 13.91Hz,

15.28Hz, 16.75Hz, 18.24Hz, 19.71Hz. The frequency doubling relationship between the frequencies corresponding to each order mode is also very obvious.

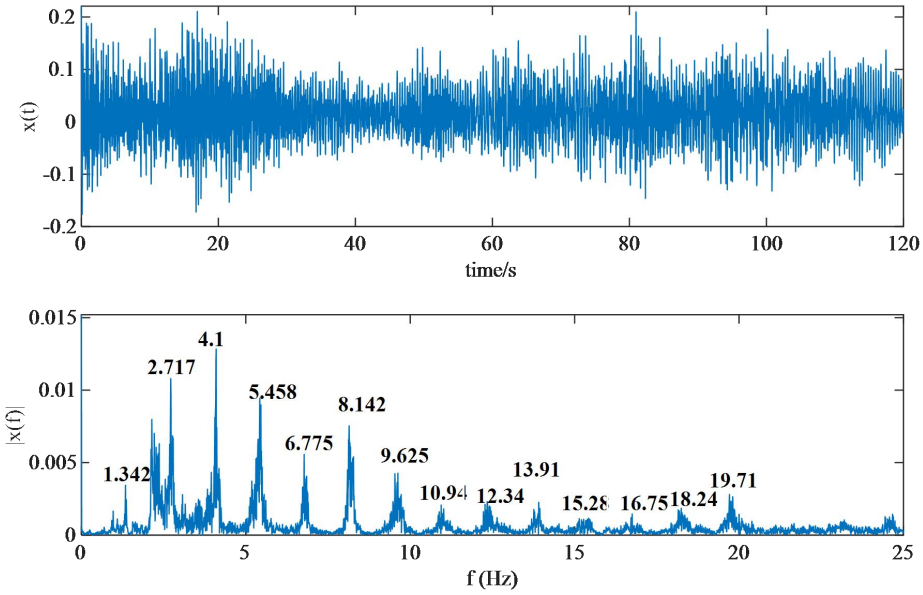

Fig.3-4 Acceleration time history chart and spectrogram

PSO-VMD analysis results of engineering signals are shown in Figure 3-5. The variation of the local minimum entropy value with the population evolution algebra in the particle swarm optimization process is shown in Figure a. Obviously, the minimum value of the local minimum entropy value 8.0432 appears in the seventh generation, and the best combination of influencing parameters $[\alpha_0, K_0] = [374, 21]$, set α = 374 and K = 21 of the VMD algorithm, and process the simulation signal. The original signal is processed by the parameter optimization variational modal decomposition algorithm to obtain 21 BIMF signals, and the spectrum diagram is further obtained by FFT. Among them, u_6 and u_7 have similar frequencies, and there is modal aliasing phenomenon, similar to u_8、u_9 and u_{19}、u_{20}. The center frequency of u_1 is close to the fundamental frequency of 1.342 Hz, but the excitation is insufficient. u_3、u_4、u_5、u_6、u_7、u_8、u_9、u_{18} are well-decomposed,

almost a single signal, which is conducive to subsequent Hilbert transform processing. In summary, although PSO-VMD has over-decomposition and modal aliasing in complex engineering signal decomposition, the overall decomposition is good, and the decomposed single signal can be used for subsequent processing.

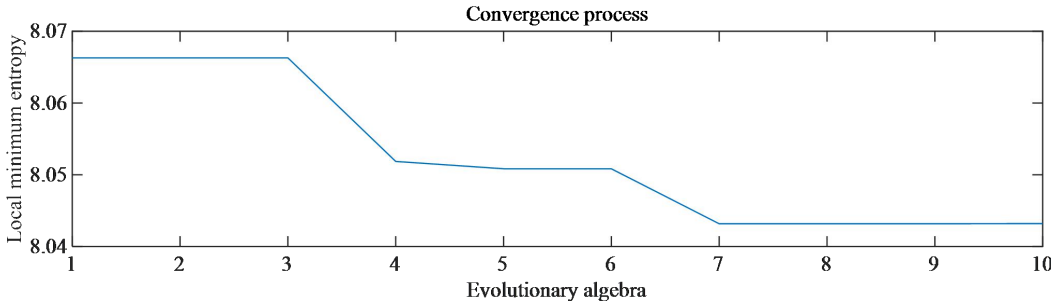

a) Change of local minimum entropy value with evolutionary algebra

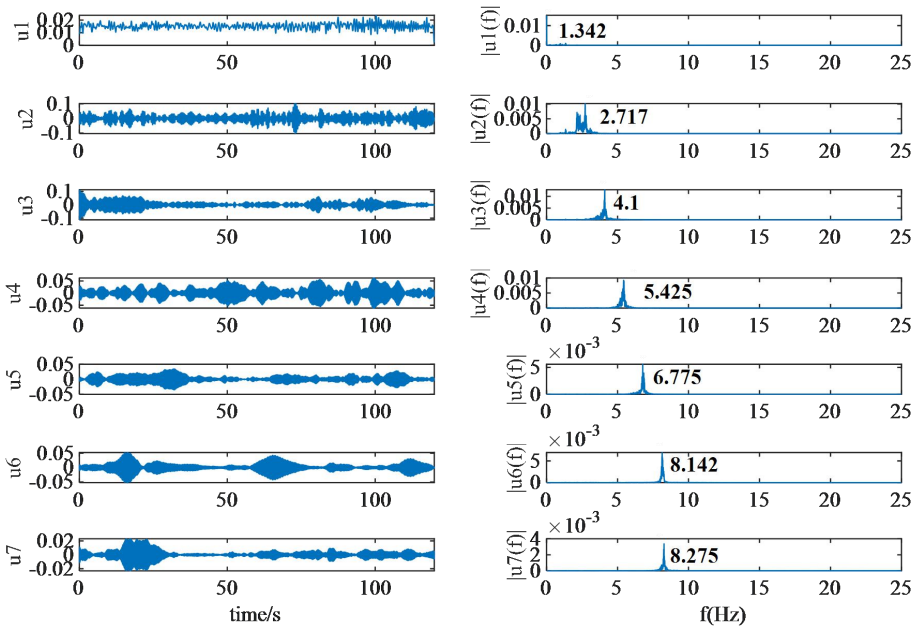

b) Time history and spectrum of u1, u2, u3, u4, u5, u6, u7

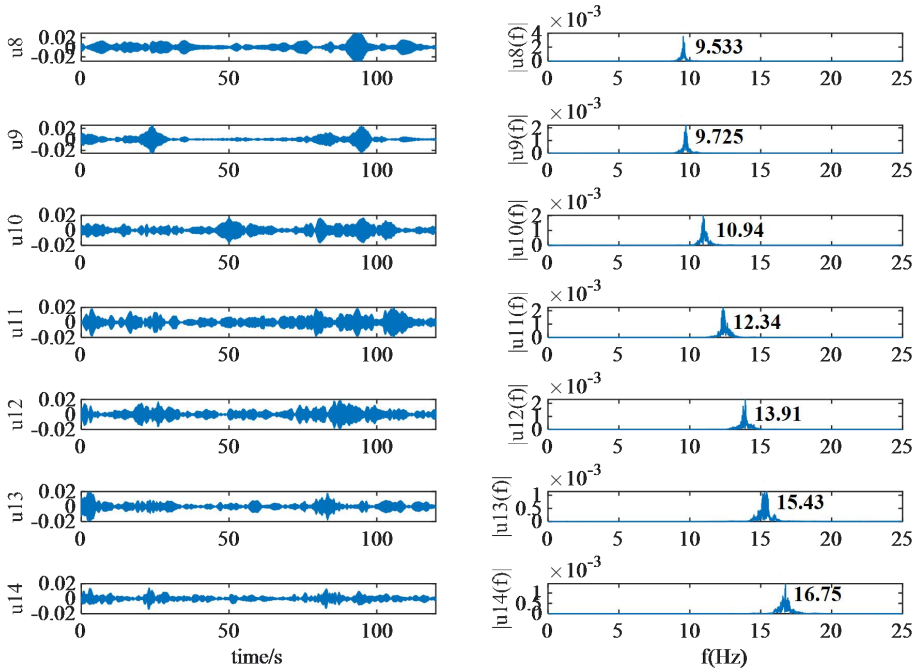

c) Time history and spectrum of u8, u9, u10, u11, u12, u13, u14

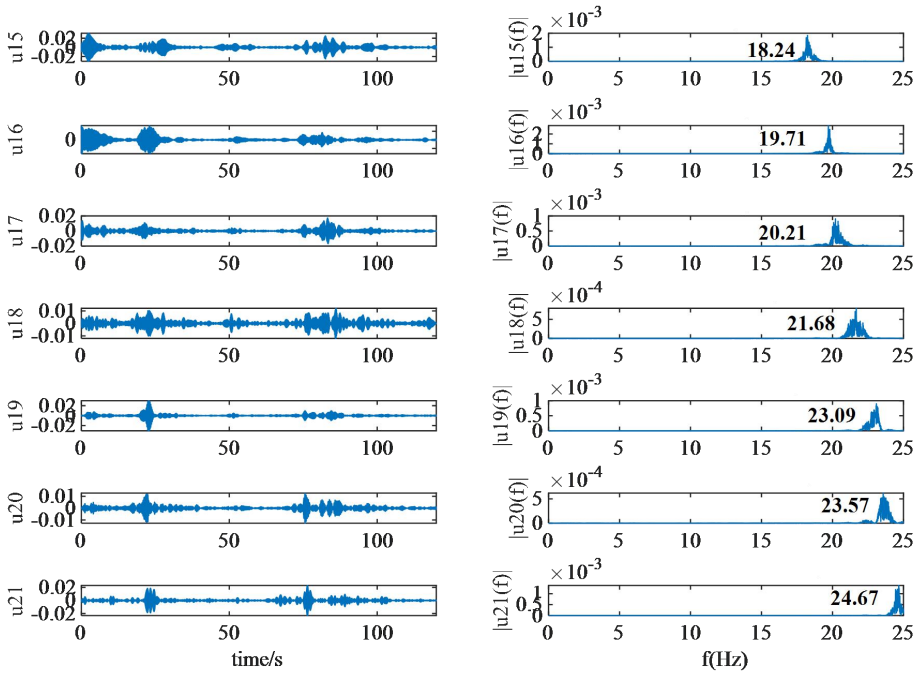

d) Time history and spectrum of u15, u16, u17, u18, u19, u20, u21

Figure 3-5 VMD analysis results of engineering signal

The processing effect of VMD is seriously affected by the penalty factor and the number of components. It is difficult to set these two parameters at the same time through subjective experience. Aiming at this problem, this chapter proposes a parallel optimization method of PSO algorithm for the key influencing parameters of VMD, and uses envelope entropy as the fitness function for optimization. The simulation signal and engineering cable acceleration signal analysis results show that, while suppressing the background noise interference of the original signal, the method can separate a good single signal component from the original signal with low signal noise. Compared with the EMD method, the analysis effect of the proposed method is better and the advantages are obvious, which is of positive significance for the promotion and application of practical engineering.

4.Time-varying cable force identification and cable model test

As of now, the most widely used method for instantaneous frequency identification is still to construct an analytical function by Hilbert transform to directly identify the instantaneous frequency of the signal. But in practical application, Hilbert transform has two limitations. First, the Hilbert transform can only be applied to narrow-band signals. The result of the Hilbert transform can only have one frequency value, that is, it can only process signals with a single frequency at any time. The VMD processing mentioned above can solve this modal aliasing problem well. The second is the impact of end effects. Sequential signals to discrete signals need to be sampled. Due to the infinite polynomials, the sampling rate for the high-frequency part (because of the infinite polynomials) is difficult to satisfy the Nyquist sampling theorem, so distortion will occur, which is the end effect. This chapter uses the signal extension method to solve the end effect. And build a time-varying cable test platform to verify the robustness of the proposed time-varying cable force identification method and the applicability of the test.

4.1 Hilbert change and instantaneous frequency

As an important modal parameter, instantaneous frequency has become a necessary means to reveal the complex time-frequency characteristics of signals and understand the mechanism of time-varying nonlinear processes. Generally speaking,the familiar frequency generally refers to the reciprocal of the signal period T:

$$\omega = \frac{1}{T} \tag{4-1}$$

According to the above definition, the frequency only exists when the entire

vibration period is complete, and the frequency is constant for the entire length of time. Therefore, the definition of traditional frequency does not reveal well the hidden feature information behind the time-varying non-stationary signals common in practical engineering.

Van der pol rigorously explored the definition of instantaneous frequency for the first time and suggested that the phase angle function be expressed It is the integral of instantaneous frequency. Subsequently, Gabor et al. [36] introduced the Hilbert transform to generate analytical signals, thereby laying the foundation for expressing instantaneous frequencies using analytical signals.

For any single component signal $x(t) = A(t)\cos\ [\Phi(t)]$, the instantaneous frequency is defined as:

$$f(t) = \frac{1}{2\pi}\frac{d\phi(t)}{dt} \tag{4-2}$$

In order to make the signal expression of x(t) unique, it is necessary to perform a Hilbert transform on the signal x(t), and the resulting analytical signal z(t) is shown in equation (4-3):

$$z(t) = x(t) + jH[x(t)]$$

(4-3)

In the formula, j is an imaginary unit; H[.] means Hilbert transform. Equation (4-4) is the polar coordinate form of the analytical signal z(t).

$$z(t) = A(t)e^{-j\phi(t)} \tag{4-4}$$

In the formula, the instantaneous amplitude A(t) and instantaneous frequency Φ(t) are defined as

$$A(t) = |z(t)| = \sqrt{x^2(t) + H^2[x(t)]} \tag{4-5}$$

$$\Phi(t) = \arctan\,[z(t)] = argtan\frac{H[x(t)]}{x(t)} \tag{4-6}$$

Simultaneous (4-2)- (4-6), the instantaneous frequency of signal x(1) can be determined by (4-7):

$$f(t) = \frac{1}{2\pi}\frac{d}{dt}\arctan \quad [z(t)] \tag{4-7}$$

4.2 Treatment and Analysis of End Effect of Instantaneous Frequency Curve

Use Hilbert transform to solve the instantaneous frequency of the signal. For the signal obtained by aperiodic or non-periodic sampling, there is an endpoint effect, that is, there is a flying wing phenomenon and exponential oscillation at both ends of the frequency. The error is the largest at both ends. Within gradually decay. Therefore, it is necessary to perform signal processing on the data at both ends to reduce the influence of errors. After the signal undergoes Hilbert transform and further solves for the instantaneous frequency, an end effect appears, as shown in Figure 4-1. In Figure 4-1(b), there are sharp and steep signals near 0 s and 4.5 s, which are generated due to the sudden start and sudden termination of the analog speed signal, and belong to the end effect of the signal after Hilbert transformation.

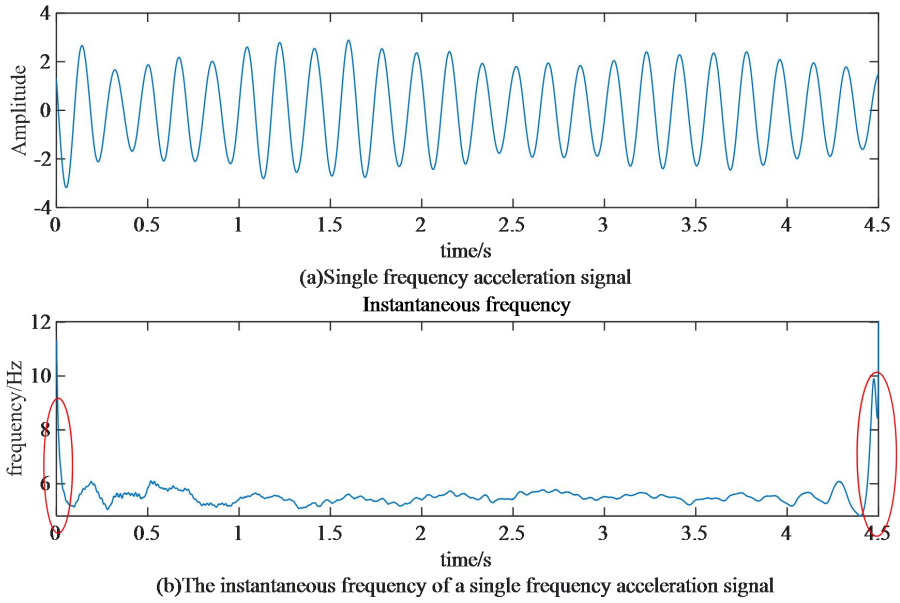

Figure 4-1 Single frequency acceleration signal and instantaneous frequency curve

For the end effect of the instantaneous frequency curve, the method of extending the acceleration signal is adopted to reduce the error of the instantaneous frequency at the end point. That is, the acceleration signal is extended by 0.25s before and after, then Hilbert and instantaneous frequency are solved, and finally the extension part is deleted. The processed acceleration signal curve and instantaneous frequency curve are shown in Figure 4-2. In Figure 4-2 (b), the instantaneous frequency value fluctuates smoothly, and there is no sharp change in the vicinity of 0s and 4.5s, which proves the feasibility and accuracy of solving the instantaneous frequency value of the signal after extension processing.

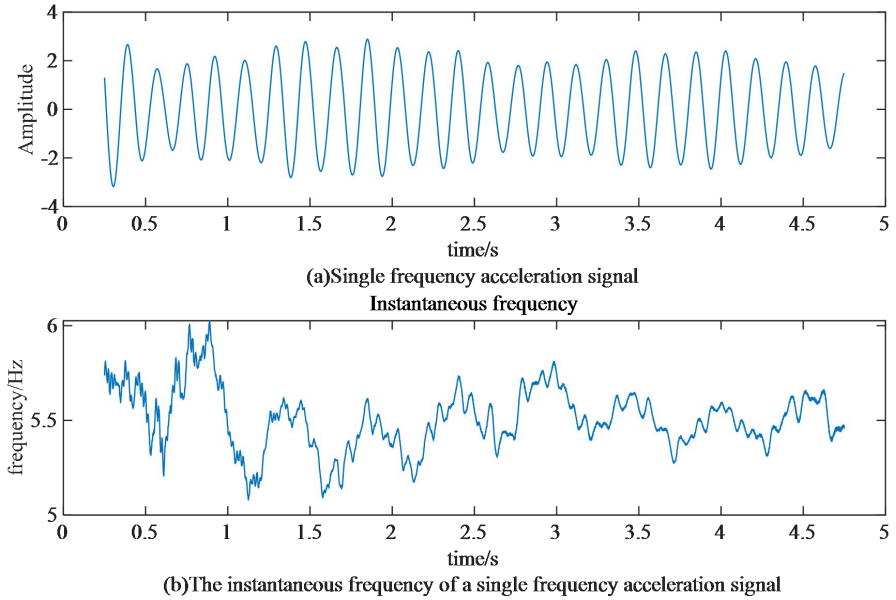

Figure 4-2 The signal curve and instantaneous frequency curve after extension processing

4.3 Cable model test

4.3.1 Test plan design

To further verify the correctness and reliability of the method in this paper in identifying time-varying cable forces, a horizontal cable vibration test platform as shown in Figure 4-3 was built. In the test, 304 stainless steel wire rope was used as the test cable. Its length, mass per unit length, diameter, initial cable force, elastic modulus, cross-sectional moment of inertia and fundamental frequency were 2.31m, 1.11 kg/m, 5mm, 589.8N, 2e +08Pa, 3.06796158e^(-11) m^4 and 2.493Hz. Before the cable force identification test, the model cable is assembled and tensioned. The initial cable force set in the test is 589.8N, and the corresponding cable fundamental frequency is 5.399 Hz. The model cable is placed horizontally, two of the bases are symmetrically fixed on the horizontal ground with four bolts, the tension of the cable

is measured by the YBY-10KN tension and pressure sensor produced by Liyang Chaoyuan Instrument Factory, and its tension is measured. The force data collection adopts the model DH3820 collector of Donghua Test Technology Co., Ltd., and the vibration modal test adopts the model DH5922 collector of Donghua Test Technology Co., Ltd. An acceleration sensor is installed at the quarter cable length to measure the vibration signal of the horizontal cable, and then the vibration signal is transmitted to the acquisition instrument. Finally, the modal analysis is performed by the Donghua test software.

In the test, the hammer is struck to make the cable vibrate. When the vibration of the cable tends to be stable, adjust the jack at one end of the cable to make the cable force change in real time and measure the real-time acceleration of the cable.

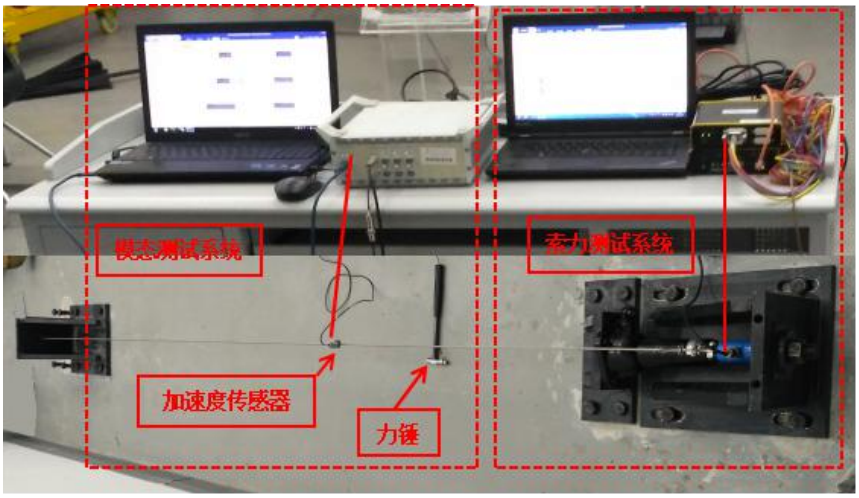

Fig.4-3 Cable vibration test platform

4.3.2 Test data analysis

A 4.5s acceleration signal is selected for testing. The sampling frequency is 1280Hz and the number of analysis points is 5760. The acceleration time history chart and spectrum chart are shown in Figure 4-4 below. It can be seen from the figure that the first few modes of the tested cable are excited, the fundamental frequency of the cable is around 5.399 Hz, and the frequency doubling relationship

between the frequencies corresponding to each mode is also very obvious.

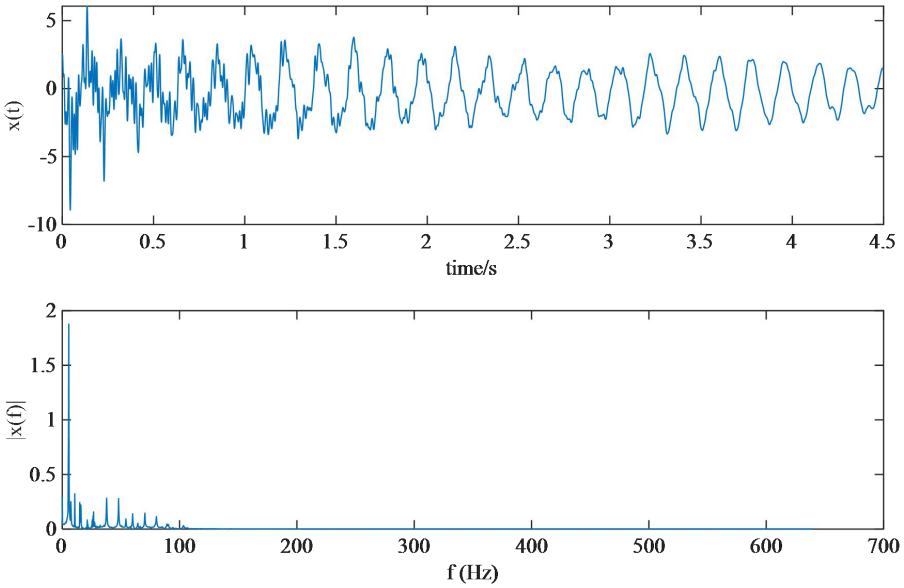

Fig.4-4 Acceleration time history chart and spectrogram

The PSO-VMD analysis results of the signal are shown in Figure 4-5. The variation of the local minimum entropy value with the population evolution algebra in the particle swarm optimization process is shown in Figure a. Obviously, the minimum value of the local minimum entropy value 6.9083 appears in the sixth generation, and the best influencing parameter combination found [α_0,K_0] =[498.4,16.4], set α=498, K=16 of VMD algorithm, and process the signal. The 16 BIMF signals obtained after the original signal is processed by the parameter-optimized variational mode decomposition algorithm are analyzed by FFT and the spectrum chart is obtained. Among them u_4 is insufficiently excited.

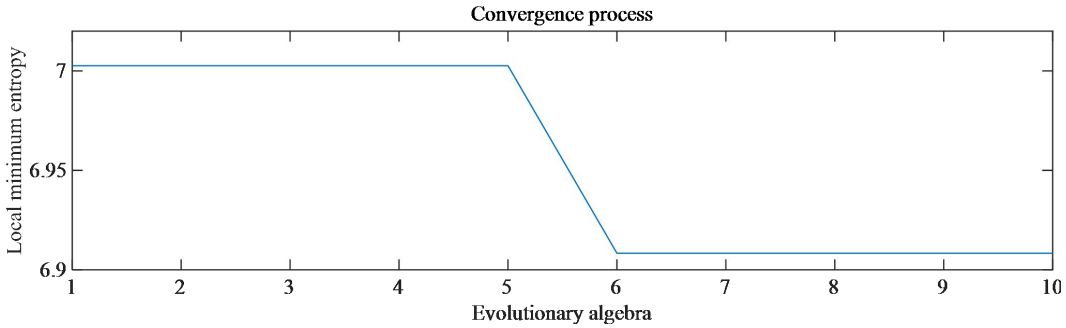

a) Change of local minimum entropy value with evolutionary algebra

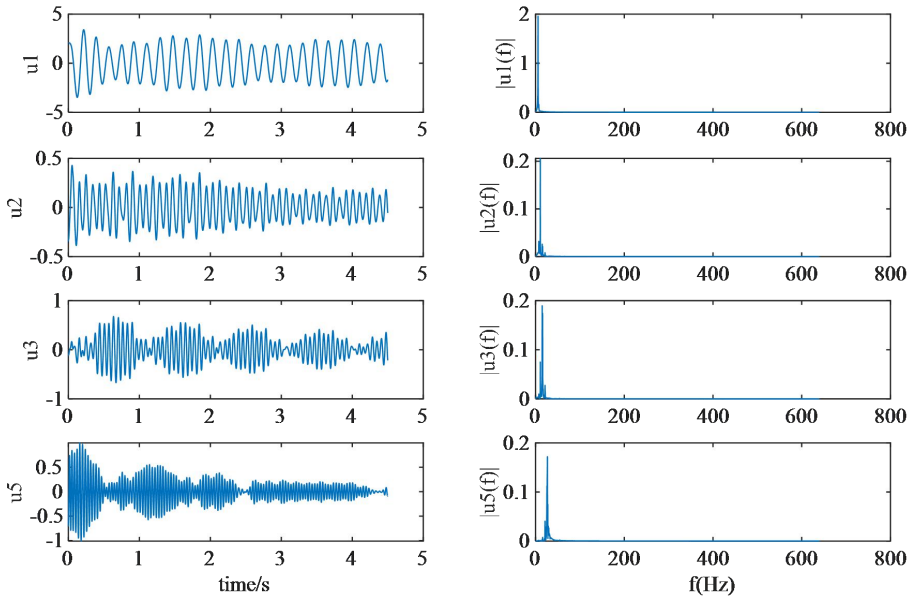

b) Time history and spectrum of u1, u2, u3, u5

Figure 4-5 Results of VMD analysis of experimental signal

Relevant research results show that if the sag of the cable is relatively small, the vibration characteristics of the cable such as frequency, array, etc., the difference between the in-plane and out-of-plane is small and can be ignored [36]. Because the cable sag used in the above test is small and the tension is relatively large, the vibration acceleration in and out of the plane measured in the test can be used to identify the cable force.

Take the first-order frequency acceleration data u1 for Hilbert transform, and extend to find the time-varying frequency, as shown in Figure 4-6. Through the vibration method formula $F = 4mL^2(\frac{f_n}{n})^2$, the instantaneous cable force is obtained. The measured cable vibration signal and the final cable force identification result and identification error are shown in Figure 4-7. The cable force identification error is calculated by equation (4-8):

$$a = \frac{||F_c(t) - F(t)||_2}{||F(t)||_2} \tag{4-8}$$

Where F_c (t) is the identified cable force F(t) is the true cable force measured by the cable force testing device. The variation range of cable force is only about 5%, which indicates that the PSO-VMD time-frequency analysis method proposed in this paper is suitable for time-varying cable force identification and has high recognition accuracy.

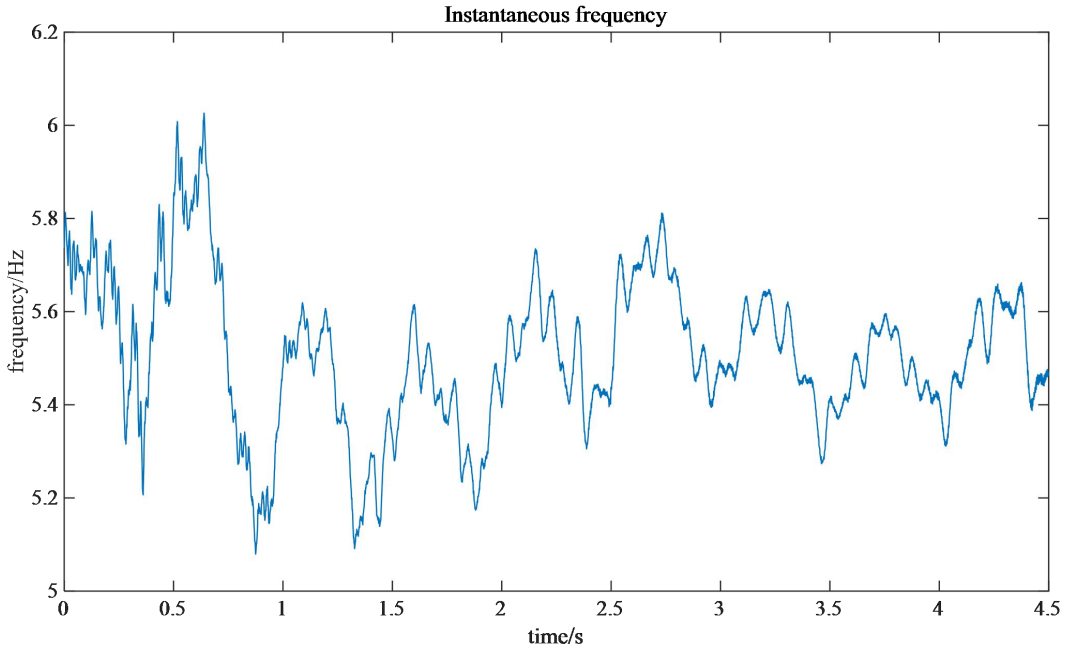

Figure 4-6 Experimental data time-frequency signal

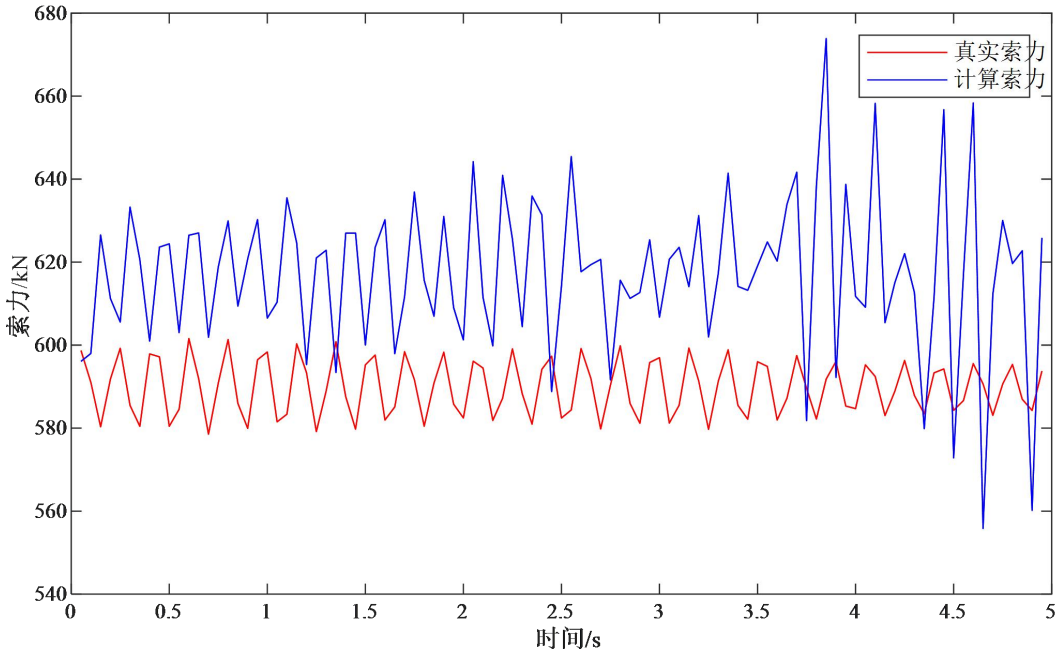

Figure 4-7 Cable force recognition result

This chapter first introduces the concept of instantaneous frequency, and then proposes a solution to the endpoint extension based on the endpoint effect of the Hilbert transform. Finally, the identification accuracy, robustness and stability of the proposed method are verified by the cable test. The main conclusions are as follows:

1. The endpoint extension method can solve Hilbert's endpoint effect well.

2. The proposed PSO-VMD time-frequency algorithm can well identify the time-varying modal frequency of the cable, and the calculated time-varying cable tension is close to the force sensor measurement with an error of about 5%. Comparing the results obtained from the HHT method and the proposed method, the results show that the latter result is more stable and the recognition error is smaller.

5. The application prospect of PSO-VMD time-frequency analysis method in marine engineering

Modal identification is very important in the field of structural health monitoring for tracking structural vibration behavior and evaluating the performance of engineering structures. Over the past few decades, modal recognition has attracted widespread attention, and many methods have been developed to extract the vibration characteristics of structures and better understand their vibration behavior. The previous method focuses on modal identification of time-invariant linear systems. However, the vibration characteristics of marine engineering infrastructure often change due to environmental influences (such as wind, waves, currents, etc.). For example, the natural frequency of a bridge across the sea may change due to temperature and humidity. The frequency of the bridge vehicle system will change as the position of the moving vehicle changes. The same change occurs on the offshore platform. When the vibration frequency approaches or reaches the natural frequency of the offshore platform, the offshore platform structure produces a significant vibration effect. For another example, a series of factors such as ship tonnage, ship type, load capacity, berth water depth, cable way, cable technical status, barge and berthing ship interaction, etc., will cause the barge mooring rope load to change in real time. In summary, it is important to understand and identify vibration characteristics (such as the frequency that changes with time), which is very useful for monitoring the operation of offshore engineering structures and identifying possible damage in the structure.

5.1 Offshore platform vibration monitoring

Offshore platform is a major infrastructure for offshore oil extraction. Long-term service is subject to the interaction of various factors such as wind and wave loads, environmental corrosion, and adhesion of marine life. With the extension of the

service time of the platform, crack damage will occur in the stress concentration or low fatigue life parts of the main structure of the platform, which will affect the stability of the platform structure. Therefore, it is particularly important to carry out structural safety inspection and evaluation of offshore platforms. The vibration detection method is a non-destructive detection method, which mainly uses the dynamic response vibration data of the measured structure to judge the parameter changes of the platform structure through the system parameter identification method, and obtains the structural damage diagnosis conclusion, and then achieves the goal of platform structure safety assessment. Since the vibration detection implementation process will not affect the normal operation of other production equipment of the platform, and can achieve long-term, online main structure damage monitoring needs, the vibration detection method has been widely used in the safety assessment research of offshore platforms.

1. Deploy acceleration sensor vibration measurement points on the crane general column, pile legs and upper deck main beam of the offshore platform.

2. Analyze the collected acceleration data by the parameter optimization variational modal decomposition method mentioned in this article to obtain the real-time changing frequency.

3. Analyze the time-varying frequency changes of each structure to further find fatigue damage such as weld cracks.

5.2 Barge mooring rope load measurement

The load mechanism of barge mooring ropes on sloped docks is quite

complicated. In addition to environmental factors such as wind, waves and currents, it is also related to ship tonnage, ship type, deadweight, berth water depth, cable way, cable technical status, barge and berth Ship interaction and a series of factors. In order to avoid serious accidents such as the cable breakage of a barge on a sloped dock, causing the barge itself to overturn or drift out of control, it is necessary to thoroughly analyze the mechanical characteristics of the barge mooring system and discuss the cable load calculation method. The vibration acceleration data of the measured cable is analyzed, and the time-varying vibration frequency is extracted using the variational modal method proposed in this paper, and the real-time load of the cable is obtained, and structural health monitoring has been achieved.

6. Conclusion

This paper proposes a time-varying cable force identification method based on parameter-optimized variational mode decomposition. The first step is to determine the optimal value of the modal number K and the balance parameter α according to the application of particle swarm optimization. The second step is to use Variational mode decomposition The measured cable acceleration signal is decomposed into a limited number of eigenmode functions. The third step is to identify the instantaneous frequency of the time-varying system through the Hilbert transform of each eigenmode function. And by considering the integer ratio of different modal frequencies to the fundamental frequency of the cable, the time-varying cable force is calculated using the vibration method formula.

The results of the cable experiment show that the time-frequency analysis method proposed by the parameter optimization variational modal decomposition can well identify the time-varying modal frequency of the cable, and the time-varying cable force calculated by the time-varying frequency is close to the force Sensor measurement. A comparison between the results obtained from the HHT method and the proposed method shows that the latter result is more stable and

the recognition error is smaller. Under experimental conditions, the relative identification error of the cable tension over time is less than 5%, which is an acceptable error for structural health monitoring.

The method mentioned in this article can also be applied to the monitoring of ocean structure health.

Reference

[1] Ou Jinping. Cumulative damage and safety assessment of major engineering structures. Chinese Mechanics towards the 21st Century—Report Collection of the 9th Young Scientist Forum of the Chinese Science Association [C]. Beijing: Tsinghua University Press 1996: 179-189.

[2] Ou Jinping. Research and application of intelligent sensing network and health monitoring system for major engineering structures [J]. China Science Foundation. 2005, (1): 8-12.

[3] Ou Jinping, Li Hui, Structural Health Monitoring in mainland China: Review and

Future Trends[J]. Structural Health Monitoring, 2010, 9(3): 219-231.

[4] Koo K Y, Brownjohn J M W, List D I, et al. Structural health monitoring of the Tamar suspension bridge[J]. Structure Control & Health Monitoring, 2013, 20(4): 609-625.

[5] Wong K-Y. Instrumentation and health monitoring of cable-supported bridges[J]. Structure Control & Health Monitoring, 2004, 11(2): 91-124.

[6] Kim BH, Park T. Estimation of cable tension force using the frequency-based system identification method. Journal of Sound and Vibration 2007;

304:660–676.

[7] Casas JR. A combined method for measuring cable forces: the cable−stayed Alamillo Bridge, Spain. Structural Engineering International 1994; 4(4):235–240.

[8] Gentile C. Deflection measurement on vibrating stay cables by non-contact microwave interferometer. NDT & E International 2010; 43(3):231–240.

[9] Kim BH, Shin HY. A comparative study of the tension estimation methods for cable supported bridges. International Journal of Steel Structures 2007; 7(1):77–84.

[10] Ren WX, Liu HL, Chen G. Determination of cable tensions based on frequency differences. Engineering Computations 2008; 25(2):172–189.

[11] Russell JC, Lardner TJ. Experimental determination of frequencies and tension for elastic cables. Journal of Engineering Mechanics 1998; 124(10):1067–1072.

[12] Humar JL. Dynamics of Structures. Prentice Hall: Upper Saddle River, NJ, 2000.

[13] Fang Z, Wang J. Practical formula for cable tension estimation by vibration method. Journal of Bridge Engineering 2012; 17:161–164.

[14] Sim SH, Li J, Jo H, Park JW, Cho S, Spencer BF Jr, Jung HJ. A wireless smart sensor network for automated monitoring of cable tension. Smart Materials and Structures 2014; 23(2):025006.

[15] Zui H, Shinke T, Namita YH. Practical formulas for estimation of cable

tension by vibration method.ASCE Journal of Structural Engineering 1996; 122(6):651–656.

[16] Liao W, Ni Y, Zheng G. Tension force and structural parameter identification of bridge cables. Advances in Structural Engineering 2012; 15(6):983–996.

[17] Cho S, Lynch JP, Lee JJ, Yun CB. Development of an automated wireless tension force estimation system for cable - stayed bridges. Journal of Intelligent Material Systems and Structures 2010; 21(3):361–376.

[18] Li H, Zhang F, Jin Y. Real - time identification of time - varying tension in stay cables by monitoring cable transversal acceleration. Structural Control Health Monitoring 2014; 21:1100–1111.

[19] Yang Y, Li S, Nagarajaiah S, Li H, Zhou P. Real - time output - only identification of time - varying cable tension from accelerations via Complexity Pursuit. ASCE Journal of Structural Engineering 2015; 142(1): 04015083.

[20] Bao Y , Shi Z , Beck J L , et al. Identification of time - varying cable tension forces based on adaptive sparse time - frequency analysis of cable vibrations[J]. Structural Control and Health Monitoring, 2017, 24(3).

[21] Huang N. E., Shen Z., Long S. R., et al. The empirical mode decomposition and the Hilbert spectrum for nonlinear and non-stationary time series analysis [J]. Proceeding of the Royal Society A, 1998, 454(1971):903-995

[22] Liu H. H., Han M. H. A fault diagnosis method based on local mean decomposition and multi-scale entropy for roller bearings [J]. Mechanism and Machine Theory, 2014, 75:67-78

[23] Dragomiretskiy K., Zosso D. Variational mode decomposition [J]. IEEE Transactions on Signal Processing, 2014, 62(3):531-544

[24] Zhao Jinping. Abnormal events Research on the influence of EMD method and its solution[J]. Qingdao Ocean University Journal,2001, 31 (6): 805-814

[25] Rilling G. Flandrin P. One or two frequencies? The empirical mode decomposition answers [J]. IEEE Transactions on Signal Processing, 2008, 56(1):85-95

[26] Flandrin P., Rilling G., Goncalves P.. Empirical mode decomposition as a filter band[J]. IEEE Signal Processing Letters, 2004, 11(2):112-114

[27] Eberhart R., Kennedy J. A new optimizer using particle swarm theory [C]. 6th International Symposium on Micro Machine and Human Science, 1995:39-43

[28] Zhang Zhonghai. Application Research on Weak Feature Detection Technology of Rolling Bearings Based on Stochastic Resonance [D]. Tianjin: Tianjin University, 2012

[29] Liu Yi. Improvement and Research of Particle Swarm Optimization Algorithm [D]. Xi'an: Xidian University, 2012

[30] Eberhart R. C. Shi Y. H. Tracking and optimizing dynamic systems with particle swarms [C]. Proceedings of the 2001 Congress on Evolutionary Computation,2001:94-100

[31] Lv Z. L, Tang B. P, Zhou Y, et al. A novel method for mechanical fault diagnosis based on variational mode decomposition and multikernel support vector machine [J]. Shock and Vibration, 2016

[32] Upadhyay A, Pachori R. B , Instantaneous voiced/non-voiced detection in speech signals based on variational mode decomposition [J]. Journal of the Franklin Institute, 2015, 352(7):2679-2707

[33] Zhang S. F, Wang Y. X, He S. L., et al. Bearing fault diagnosis based on variational mode decomposition and total variation denoising [J]. Measurement Science and Technology, 2016, 373:325-339

[34] Zhang S. F, Wang Y. X, He S. L., et al. Bearing fault diagnosis based on variational mode decomposition and total variation denoising [J]. Measurement Science and Technology, 2016, 373:325-339

[35] Jiang Yonghua, Tang Baoping, Liu wenyi, et al. Feature extraction method based on Parameter Optimized Morlet wavelet transform [J]. Chinese Journal of Scientific Instrument, 2010, 31(1): 56-60